atmosphere

MDPI

Article

Geochemistry and Provenance of Loess on the Miaodao Islands, China

Yunfeng Zhang [1], Kuifeng Wang [2,3,*], Jianchao Song [2], Paul Liu [3], Chuanbo Xia [2], Muhammad Risha [3], Xiaohua Qiu [2], Yan Xu [2], Minghui Lv [1], Kuifeng Gao [1] and Lin Wang [1]

[1] 801 Institute of Hydrogeology and Engineering Geology, Shandong Provincial Bureau of Geology & Mineral Resources, Shandong Engineering Research Center for Environmental Protection and Remediation on Groundwater, Jinan 250014, China

[2] Shandong Institute of Geological Sciences, Key Laboratory of Coastal Science and Integrated Management, Key Laboratory of Gold Mineralization Processes and Resource Utilization, Ministry of Natural Resources, Shandong Key Laboratory of Geological Process and Resource Utilization in Metallic Minerals, Shandong Yellow River Basin Soil Remediation Technology Innovation Center, Shandong Engineering Technology Collaborative Innovation Center of Coastal Evaluation and Planning, Jinan 250013, China

[3] Marine, Earth and Atmospheric Sciences Department, North Carolina State University, Raleigh, NC 27695, USA; jpliu@ncsu.edu (P.L.); mrisha@ncsu.edu (M.R.)

* Correspondence: maplewkf@126.com

Abstract: Loess deposits are widely distributed across the globe and provide detailed records of climatic changes since the Quaternary period. Their geochemical element characteristics are important indicators of paleoenvironmental evolution and provenance. Therefore, four typical loess sections from four different islands of the Miaodao Islands were selected for systematically geochemical analysis of major and trace elements. The geochemical data of major and trace elements are very similar, indicating that the loess of all islands on the Miaodao have a common provenance. The geochemical test results show that t SiO_2, Al_2O_3, Fe_2O_3 and CaO are the major chemical components of loess, with an average total content of 85–90%. The average Eu/Eu*, ΣLREE/ΣHREE, La_N/Yb_N, Gd_N/Yb_N values of the Miaodao Islands loess range from 0.65 to 0.69, 7.84 to 8.31, 8.02 to 9.99, 1.40 to 1.76. These data are similar to and different from those of the Chinese Loess Plateau, indicating the diversity of Miaodao Islands Loess provenance. The CIA (Chemical Index of Alteration) (50–65) and Na/K results suggest that the loess here had experienced incipient chemical weathering. The A-CN-K (Al_2O_3-CaO* + Na_2O-K_2O) diagram indicates that the weathering trend of the loess sections is consistent with that of continental weathering. The local loess data points are close and parallel to the A-CN line, suggesting that the loess dust material on the Miaodao Islands originated from the extensive upper continental crust, and was highly mixed in the process of wind transport and deposition. The relationships of Log[(CaO + Na_2O)/K_2O] versus Log(SiO_2/Al_2O_3), Na_2O/Al_2O_3 versus K_2O/Al_2O_3, LaN/YbN versus Eu/Eu*, Sc-Th-La and Zr-Sc-Th plots of major and trace elements reveal that the loess sources for the Miaodao Islands are similar to those of the Loess Plateau, which were derived from alluvial fan deposits flanking the Qilian Shan in China, the Gobi Altay and Hangayn Mountains in Mongolia. However, the loess of the Miaodao Islands is coarser in average grain size and contains abundant marine fossils, with gravel layers, indicating it is allochthous and near-source, which suggests it mainly originated from the adjacent exposed sea floor sediments of the Bohai Sea during glacial periods. Finally, we conclude that the loess of the Miaodao Islands is the result of a gradual accumulation process, in which the relative amount of distant-source material decreased and the near-source material increased in response to changes in sea level and paleoclimate. Our findings support that the loess of the Miaodao Islands was formed by mixing material from distant and proximal sources.

Keywords: loess; Miaodao Islands; major and trace elements; geochemical; provenance

check for updates

Citation: Zhang, Y.; Wang, K.; Song, J.; Liu, P.; Xia, C.; Risha, M.; Qiu, X.; Xu, Y.; Lv, M.; Gao, K.; et al. Geochemistry and Provenance of Loess on the Miaodao Islands, China. *Atmosphere* **2024**, *15*, 261. https://doi.org/10.3390/atmos15030261

Academic Editor: Paul V. Doskey

Received: 28 December 2023
Revised: 1 February 2024
Accepted: 10 February 2024
Published: 22 February 2024

1. Introduction

Loess is widely distributed around the world, accounting for about 10% of the earth's surface area [1]. It records Quaternary climate change, which is of great significance to understanding the ancient atmospheric circulation model and reconstructing paleoenvironmental conditions [2–11]. Loess deposits reflect processes of dust material transportation, accumulation, and post-sedimentary alteration. The migration, enrichment, and re-combination of chemical elements record the changes in the climatic environment throughout the formation process. The concentrations and combination characteristics of chemical elements in loess strata could effectively reveal the intensity of chemical weathering and the evolution of paleoclimate conditions [12–16]. Furthermore, the different chemical elements and related parameters were also used to identify the sources of loess dust to a certain extent [17–20]. Trace elements are traditionally defined as elements with 1% and less than 0.1% of rock mineral content. Due to their stable chemical properties, they are used to explore sedimentary types and their sedimentary environments. Trace elements and their ratios are significant in the study of changes in the paleoclimate and the paleoenvironment [21,22]. Trace elements have an important role in determining the source of sedimentary rocks, as these trace elements are mainly enriched in certain minerals, such as Zr and Hf in zircon. As one of the important indicators for loess source discrimination, chemical weathering intensity analysis, and paleoclimate environment evolution, elemental geochemistry has been widely used in the study of aeolian accumulation [19,23–25]. China has one of the most extensively developed loess deposits in the world. The loess in China is different from those in Europe and in the United States [7,13,15,19], where they were mainly glacial environments. Previous studies mainly focused on the loess plateau, located in Central China (CLP), but in recent years, research on its periphery has gradually increased and achieved certain progress [26–31]. One example is the study of the loess on the Miaodao Islands located near the coast of Eastern China. The Miaodao Islands are found between the Bohai Sea and the Yellow Sea in the northern Jiaodong Peninsula, China (Figure 1). Although the scale is not large, the loess on the Miaodao Islands is in a special position influenced by sea–land interactions and contains marine fossils, which more sensitively recorded the dramatic climate change over the late Pleistocene [10]. Since the 1960s, it has been attracting the attention of scholars [32]. Previous studies have mainly discussed the loess strata, grain size, magnetic susceptibility, geochemical parameters, and paleontology in this area [33–39]. It is generally believed that the loess of the Miaodao Islands mainly accumulated during the last glacial period roughly during a period of 100,000 years, under the influence of dramatic sea level changes and harsh cold and dry environments [40–42]. However, the provenance of loess in Miaodao Islands has always been controversial. One theory suggests nearby sources [43–45] while the other is in favor of a combination of a proximal and distal sources [9,38,46]. For loess deposits of Miaodao Islands different hypothesis on particle sources have been proposed, but none of them has been tested using a comprehensive geochemical approach yet. We aim to provide a first raw geochemical characterization of selected layers from this succession in order to explore the potential provenance(s) of the sediment material. Our purpose is to identify potential local and remote particle sources, and thus to test current hypothesis on the origin of loess deposits and aeolian deposition over Miaodao Islands. Moreover, our data increase the geochemical picture of the Miaodao Islands loess deposits, for which this characterization is generally rather poor, in contrast to the more abundant data of Western China, such as the Loess Plateau data currently available. This paper aims to analyze the trace elements geochemistry of loess deposits of Miaodao Islands and compare them in detail with those of the CLP and the main potential source areas. It will have significant implications on the changes in the paleo-environment of the Miaodao Islands area.

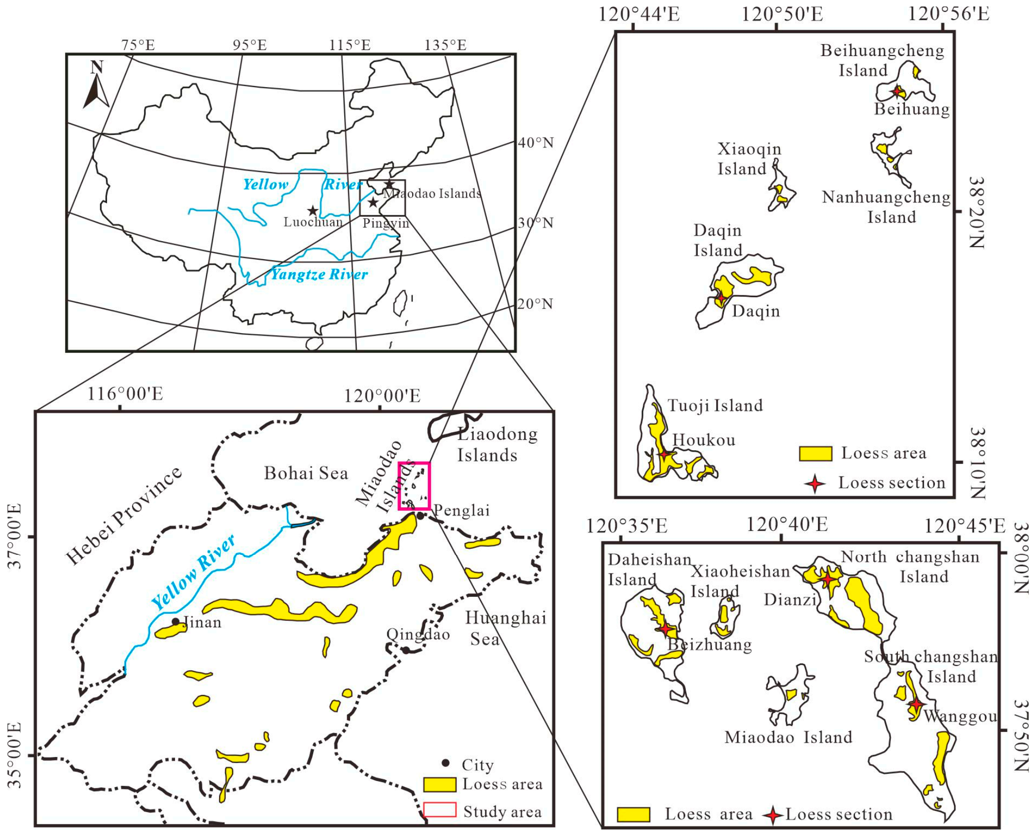

Figure 1. The location and distribution of the main Miaodao Islands.

2. Materials and Methods

2.1. Study Area

The Miaodao Islands, also known as the Changshan Archipelago, were formerly under the jurisdiction of Yantai's Changdao County. They are now part of the Yantai Changdao Marine Ecological Civilization Comprehensive Experimental Zone. The islands are separated from the Penglai City area by the sea to the south, facing the Yellow Sea to the east, adjacent to the Bohai Sea to the west, and opposite to Dalian in the north. The archipelago consists of 151 islands of various sizes, with a total area of 56.8 km^2, and is arranged in a northeast-southwest direction (Figure 1).

The Miaodao Islands are located at the junction of the Jiaoliao platform uplift, with exposed strata of the Penglai Group of the Neoproterozoic Sinian System. They are composed of low-grade metamorphosed rocks, such as quartzite, slate, and schist. The overall structure is monoclinal and the topography is relatively gentle. Magmatic rocks are only exposed in a small amount, including the Mesozoic diorite porphyry at Bawang Mountain on Tuoji Island, and a certain area of Cenozoic black basalt [47] is exposed in the west of Daheishan Island. The geology of the area is mainly faulted, which can be divided into three groups according to direction: NNE, NEE, and NNW, followed by some small folds, mostly interlayer folds.

The islands range from 10 to 70 m in elevation, with loess covering most of them, with a total area of 11.3 km^2, accounting for about 20% of the islands area. The loess can be divided from bottom to top into lithic loess, marl loess, and Holocene loess [37,38], mainly exposed in ancient gullies and gentle slopes on the islands. The thickest loess is located in the valleys, and its accumulation distribution has obvious inheritance to the original landform (Figure 2). Some loess are in direct contact with the underlying bedrock, some are covered by beach gravel layers, and some are in transition with red clay. From the exposed sections, the upper part is light yellow and the lower part is reddish brown. In some areas, there are 1–3 paleosol (ancient soil) layers. The upper loess is loosely cemented and vertically jointed. Calcareous nodules or calcareous mycelia are often found in the middle and upper parts of the loess layer, with different sizes and shapes, mostly scattered, and arranged in some discontinuous layers. The loess landforms mainly include loess sea cliff, loess gully, loess platform, and loess slope, etc. Before the loess accumulation, the surface was mainly affected by water and coastal erosion, forming valleys and coastal landforms. After the loess accumulation, the valleys were filled, the coastal terraces were buried, and the current unique loess landforms were formed by continuous cycles of water-erosion-accumulation.

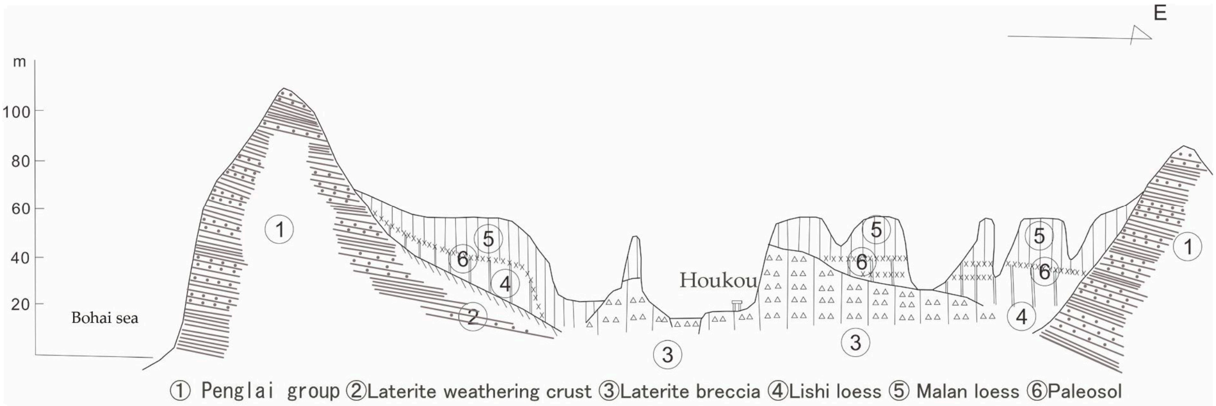

Figure 2. The loess section of Houkou village of Tuoji Island (modified from [38]).

2.2. Comparison of Loess Profiles in Miaodao Islands

Through our OSL sample testing of BZ section, and comparing the loess profile in this study with the previous Miaodao loess strata [40–42,44,46,48], we can see that the Miaodao loess was mainly sedimented since the late Pleistocene (Figure 3). Due to artificial activities and the natural factors such as the increase in sea levels and surface erosion, the Holocene strata in the Miaodao loess were missing [40].

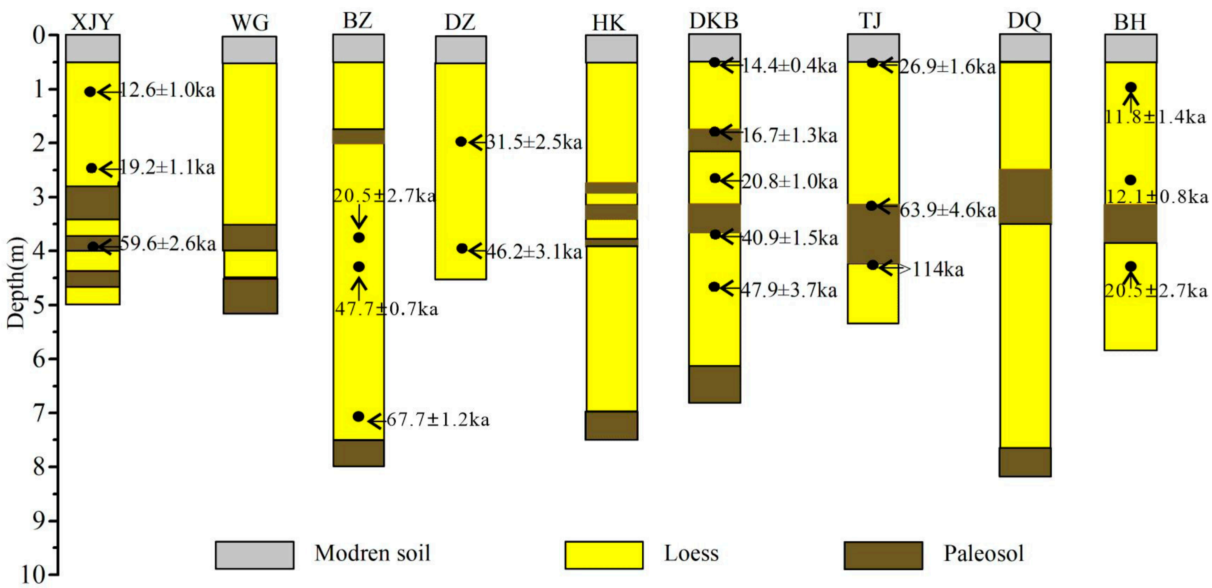

Figure 3. OSL stratigraphic comparison of the loess profile in Miaodao Islands (The OSL age of XJY profile from [42]; the OSL age of DZ profile from [46]; the OSL age of DKB profile from [40]; the OSL age of TJ profile from [10]; the OSL age of BH profile from [41]; the OSL age of BZ profile from this study).

2.3. Loess Section and Sampling

Based on the preliminary field investigation, four typical loess sections were selected for geochemical analysis sampling. These sections are located in Dianzi of North Changshan Island, Wanggou of South Changshan Island, Beizhuang of Daheishan Island and Houkou of Tuoji Island where loess sediments are widely distributed, complete, and easy to collect. Samples were taken from bottom to top in a 10 cm intervals, including surface soil, loess, paleosol, plant debris, and calcareous nodules, and stored in well-sealed plastic bags. In total, 256 samples were collected, including 46 from Dianzi, 51 from Wanggou, 81 from Beizhuang, and 78 from Houkou. The specific geological characteristics of sampling locations and profiles are shown in Table 1, and Figures 4 and 5.

Table 1. Sampling locations and geological features of loess sections.

Sampling Site	Coordinate Position	Sedimentological Characteristics of Loess Section
Dianzi Village West, North Changshan Island (DZ), Figure 4a	E: 120°41′10.54″ N: 37°59′09.30″	The loess section is 5.0 m high, consisting of bedrock, and loess from bottom to top. Yellow loess, more voids, occasionally quartz breccia, lower soil compaction, upper vertical joint development, loose cementation, easily broken.
Southwest of Wanggou Village, South Changshan Island (WG), Figure 4b	E: 120°44′20.12″ N: 37°55′58.68″	The loess section is 5.2 m thick, with bedrock at the bottom and farmland at the top. Silty clay at the bottom of loess, reddish brown, central 2–3 m range, the development of a layer of ginger calcareous nodules and white calcareous hyphae, layered intermittent arrangement, upper vertical joint development, pale yellow.
Beizhuang Village, Daheishan Island (BZ), Figure 4c	E: 120°37′08.48″ N: 37°57′52.21″	The loess section is 9.2 m high, and a layer of grayish-brown paleosol is embedded at 5.5–5.95 m. The top vegetation is lush and covered with a large amount of artificial landfill and miscellaneous soil. The upper part of the loess has developed vertical joints, loose cementation and easily collapsed. The middle and lower part of the loess blocks has a high hardness, and a large number of collapsed loess is accumulated at the bottom. Locally exposed bedrock is Cenozoic black basalt.
Houkou Village South, Tuoji Island (HK), Figure 4d	E: 120°44′48.71″ N: 38°10′36.26″	The loess profile is 8 m high, and there are three layers of reddish-brown paleosol layer in the middle. The top vegetation is lush, the bottom bedrock is exposed, and the bedrock breccia is seen. The upper part of the loess reveals vertical joint development, loose cementation, easy to collapse, the lower part of the loess is solid, the upper part of the loess is light yellow, the lower part of the reddish brown.

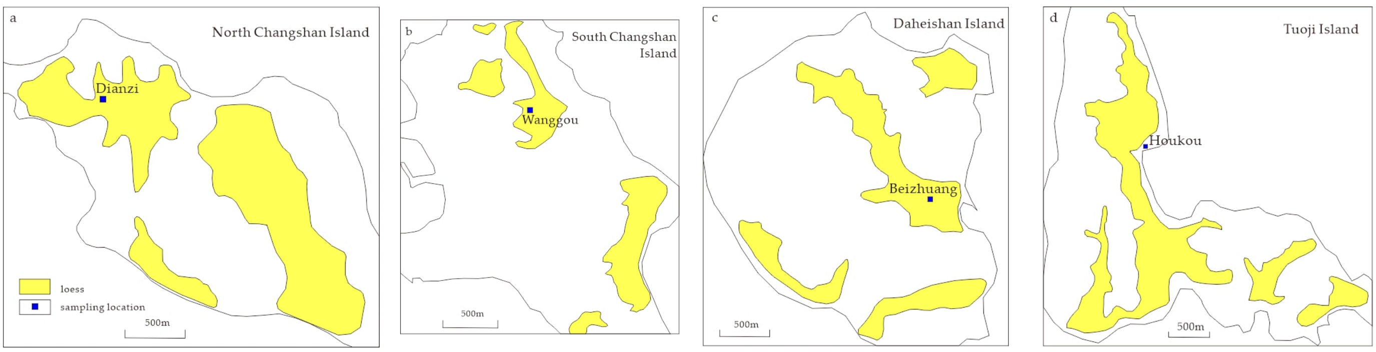

Figure 4. The sketch map of loess and locations of sampling islands.

Figure 5. The geological features and sample locations of loess sections.

2.4. Analysis Method

Geochemical analysis of the samples were completed at the Key Laboratory of Ore-forming Processes and Mineral Resources Utilization, Natural Resources Department, Shandong Institute of Geological Sciences. SiO_2 and Al_2O_3, and other major elements, were measured using a Rigaku Primus II X-ray Fluorescence Spectrometer. The process involved placing the sample in a plastic compression ring on a flat pressing mold, pressing it at 30 MPa on a powder pressing machine, and then directly testing it with the X-ray Fluorescence Spectrometer. The element compositions were calculated based on the fluorescence intensity, and the spectrum line interference was calibrated using the empirical coefficient method. CaO, MgO, Fe_2O_3, Mn, Ti, Na_2O, K_2O, P, and V were measured using a Thermo Fisher iCAP 7600 Inductively Coupled Plasma Optical Emission Spectrometry (ICP-OES). The process involved decomposition of 0.1 g samples with 2 mL concentrated nitric acid, 2 mL hydrochloric acid, 1 mL hydrofluoric acid, and 1 mL perchloric acid, evaporating the perchloric acid smoke for 3 h on an electric heating plate, dissolving the residue with 2 mL hydrochloric acid, transferring it to a 25 mL plastic test tube, and then testing the solution with ICP-AES. Rare earth elements and other trace elements were analyzed using a Thermo Fisher X Series II Inductively Coupled Plasma Mass Spectrometer (ICP-MS), but the analysis process was different. Specifically, for rare earth elements, the 0.05 g sample was dissolved in 1 mL concentrated hydrofluoric acid and 0.5 mL nitric acid under high temperature and high pressure in a closed sample dissolver for 24 h, the residue was dissolved in hydrochloric acid and nitric acid (3:1), transferred to a polyethylene test tube, and then diluted and analyzed directly with ICP-MS. For trace elements, the 0.1 g sample was decomposed with 10 mL nitric acid, 10 mL hydrofluoric acid, and 2 mL perchloric acid, and the perchloric acid was evaporated for 4 h. The residue was dissolved in hydrochloric acid and nitric acid (3:1), transferred to a polyethylene test tube, and then diluted and tested directly with ICP-MS. All chemical elements and indexes testing data of loess on the Miaodao Islands can be seen in detail in the Supplementary Table S1.

3. Results and Discussion

3.1. Major Elements

The enrichment of the major elements in loess reflects the main mineral composition of the sediment. A large number of studies have shown that the most common minerals in loess are quartz, plagioclase, potassium feldspar, green mica, hornblende, feldspar, kaolinite, and clay minerals [49–51]. There are more than 30 kinds of minerals in the loess of Miaodao Islands, among which quartz, feldspar, calcite and other light minerals are the main ones, with a proportion of 96.7–97.8%, while heavy minerals only account for 2.92–3.3%. The contents of common hornblende, epidote and limonite are the highest in heavy minerals. The clay minerals are mainly illite, followed by kaolinite, chlorite and montmorillonite [38,52–54].

Based on the major element data (Tables 2 and 3, Figures 6 and 7), SiO_2, Al_2O_3, Fe_2O_3 and CaO are the major chemical components of loess, with an average total content of 85–90%. Other oxides with a content exceeding 1% include MgO, Na_2O, and K_2O. The constant element composition of loess in each section is the same, and the numerical range is similar. The average content of SiO_2 is 67–69%, which is similar to that of Pingyin loess and higher than the average values of Luochuan loess and upper continental crust (UCC) [21,40,55,56]. The high content of SiO_2 mainly comes from quartz, and feldspar and clay minerals also contribute a certain proportion. The average content of Al_2O_3 is higher than that of Pingyin loess except for Dianzi, but lower than that of Luochuan and upper continental crust. The average content of Fe_2O_3 is lower than that of Pingyin loess, Luochuan, and upper continental crust (UCC) (Tables 2 and 3), but the difference with Pingyin loess is small. The fluctuation curves of Al_2O_3 and Fe_2O_3 are positively correlated, which is due to the relative enrichment of Al and Fe in clay minerals, while the curves of Al_2O_3 and Fe_2O_3 compared with SiO_2, the Wanggou section shows extreme similarity, while the Beizhuang section shows obvious opposite. The content of MgO is mostly between 1 and 2%, which is similar to that of Pingyin loess, but lower than that of Luochuan and UCC. In the Beizhuang section, the fluctuation curves of MgO, Al_2O_3, and Fe_2O_3 are similar, and the highest value of Fe_2O_3 is higher than that of other sections, which may be related to the basalt distributed in the western part of the Daheishan Island affecting the chemical composition of loess. The average content of CaO is much higher than that of Luochuan, lower than that of Pingyin loess, and lower than that of UCC except for Dianzi. Compared with other constant elements, the fluctuation range of CaO is the largest, which is consistent with the distribution of calcium nodules and fungal filaments. Within a certain range below the paleosol of Beizhuang and Houkou, the CaO content is obviously concentrated, which may be related to the syndepositional leaching of carbonate minerals. The average content of Na_2O and K_2O is close to Pingyin, lower than Luochuan and UCC.

Table 2. The content of major elements in the loess section of Miaodao Islands and other typical sections.

Location	Sample Quantity	Distribution	SiO_2	Al_2O_3	Fe_2O_3	MgO	CaO	Na_2O	K_2O	Data Sources
Dianzi	46	maximum value	71.81	11.49	3.61	1.45	6.36	2.23	2.49	This test
		minimum value	65.65	9.79	2.88	1.18	3.19	2.01	2.24	
		mean value	68.89	10.75	3.29	1.31	5.12	2.09	2.36	
		coefficient of variation	2.10	2.60	5.40	5.20	15.80	2.30	2.80	
Wanggou	51	maximum value	71.36	16.35	5.68	1.57	7.45	2.15	2.76	
		minimum value	62.20	11.89	3.92	1.21	1.01	1.41	2.18	
		mean value	67.64	13.85	4.76	1.42	2.59	1.89	2.49	
		coefficient of variation	3.70	8.90	10.10	4.80	74.90	9.90	5.10	
Beizhuang	81	maximum value	73.02	16.42	7.35	2.80	4.61	2.54	3.02	
		minimum value	58.55	11.41	3.78	1.30	1.21	1.52	2.33	
		mean value	68.02	13.13	4.74	1.73	2.40	2.11	2.69	
		coefficient of variation	5.60	10.20	20.40	22.20	36.70	10.50	5.60	
Houkou	78	maximum value	71.15	15.60	5.98	1.91	7.54	2.42	2.96	
		minimum value	61.84	10.80	3.47	1.13	0.79	1.55	2.32	
		mean value	67.04	13.14	4.62	1.53	3.10	2.14	2.66	
		coefficient of variation	3.30	10.90	16.20	9.90	76.30	8.00	6.40	
Pingyin	70	mean value	69.28	11.94	4.00	1.44	7.76	2.27	2.68	[56]
XiaShu	54	mean value	68.07	13.32	5.3	1.61	1.00	0.92	2.35	[57]
Luochuan	12	mean value	66.40	14.20	4.81	2.29	1.02	1.66	3.01	[55]
Upper continental crust (UCC)		mean value	66.00	15.20	5.00	2.20	4.20	3.90	3.40	[21]

Table 3. Regional averages of major and trace elements in loess and average loess compositions.

Locality	SiO_2	TiO_2	Al_2O_3	FeO	MnO	MgO	CaO	Na_2O	K_2O	P_2O_5	Rb	Sr	Ba	Pb	Th	Zr	Nb	La	Ce	Y	Sc	V	Cr	Ni	Cu	Zn	Ga
DZ	68.89	0.53	10.75	2.96	0.06	1.31	5.12	2.09	2.36	0.07	82.52	194.63	512.97	18.80	8.75	149.57	10.74	27.57	52.56	21.60	8.12	60.70	47.93	20.20	15.58	48.44	15.55
WG	67.64	0.73	13.85	4.28	0.08	1.42	2.59	1.89	2.49	0.06	96.34	153.25	526.96	22.01	11.29	206.79	13.95	33.37	68.85	26.37	10.35	86.81	60.53	28.04	21.43	58.05	18.06
BZ	68.02	0.70	13.13	4.27	0.07	1.73	2.40	2.11	2.69	0.12	97.36	170.92	515.61	20.77	10.38	186.80	12.96	33.14	63.88	27.26	9.98	84.40	59.52	26.00	20.65	80.57	17.10
HK	67.04	0.72	13.14	4.16	0.07	1.53	3.10	2.14	2.66	0.07	113.11	177.74	551.68	22.59	11.44	220.38	14.18	36.29	69.95	29.18	10.12	82.03	58.72	27.08	21.66	68.09	18.52
LC	65.69	0.7	13.13	4.38	0.1	2.36	8.86	1.66	2.51	0.16	89	215	457	18	10.9	181	11.7	30.3	62.6	25.5	11.9	99	69	34	30	78	17
XS	68.07	0.81	13.32	5.3	0.09	1.61	1.00	0.92	2.35	0.18	—	108.78	492.46	—	17.18	—	—	—	—	—	—	117.32	80.69	41.15	46.86	95.32	19.14
PY	69.28		11.94	4.00		1.44	7.76	2.27	2.68	—	35.69	88.61	295.56	3.02	—	138.82	—	—	—	—	—	—	64.09	9.03	1.57	16.42	—
CLP	62.89	0.58	12.59	4.33	0.09	3.84	10.91	1.67	2.32	—	101	246	409	20	12.7	221	13.1	35.7	71.4	27.4	11.7	—	—	—	—	—	16
GAL	70.71	0.71	11.74	3.75	0.07	2.15	6.67	1.68	2.22	0.14	79	208	427	15	9	322	14	29	61	26	—	79	67	27	19	57	12

Major oxides are in wt%, trace elements in ppm. Total iron expressed as FeO. Major element data are recalculated on a volatile-free basis.

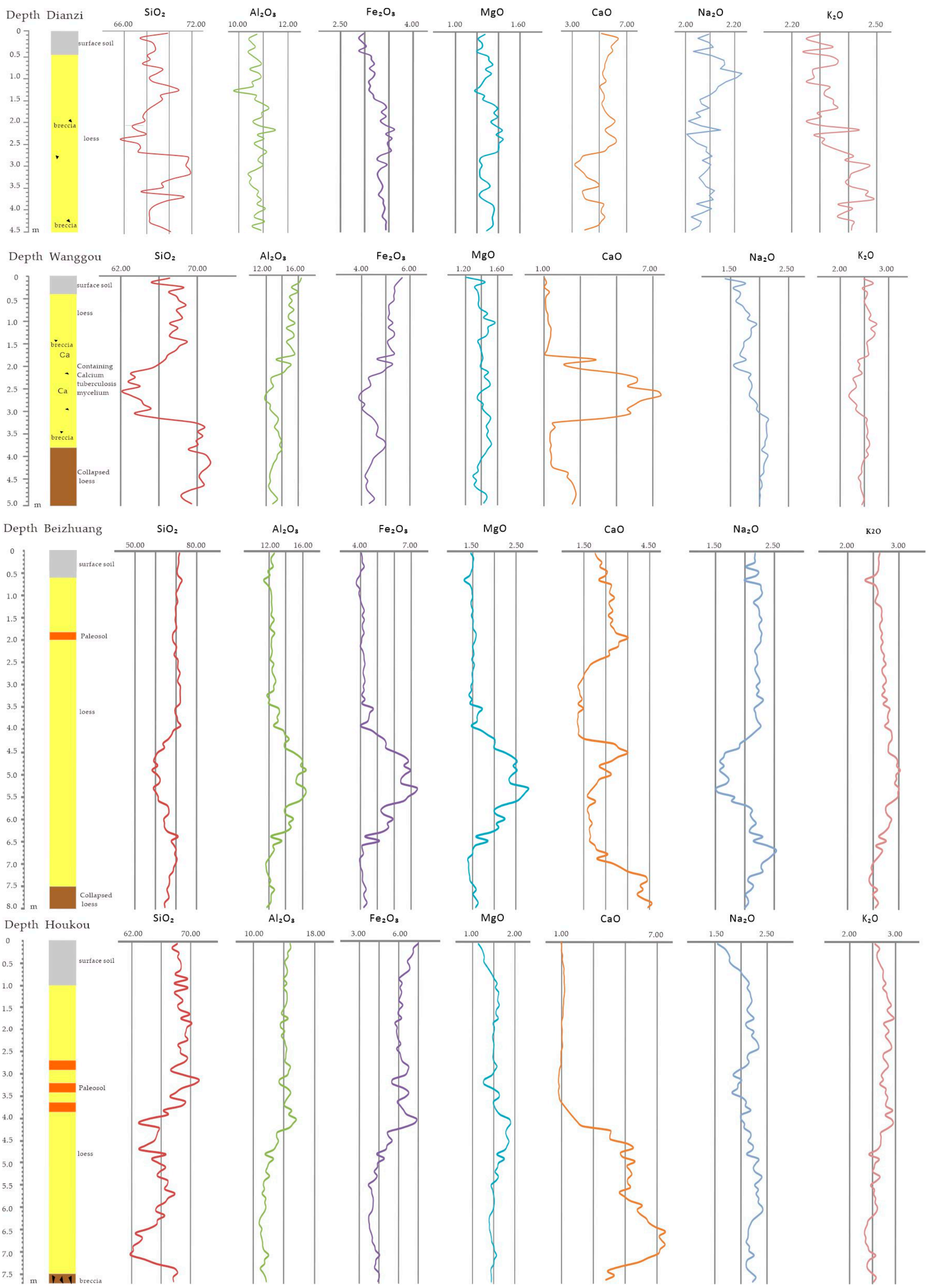

Figure 6. Variation curves of loess major elements as a function of depth.

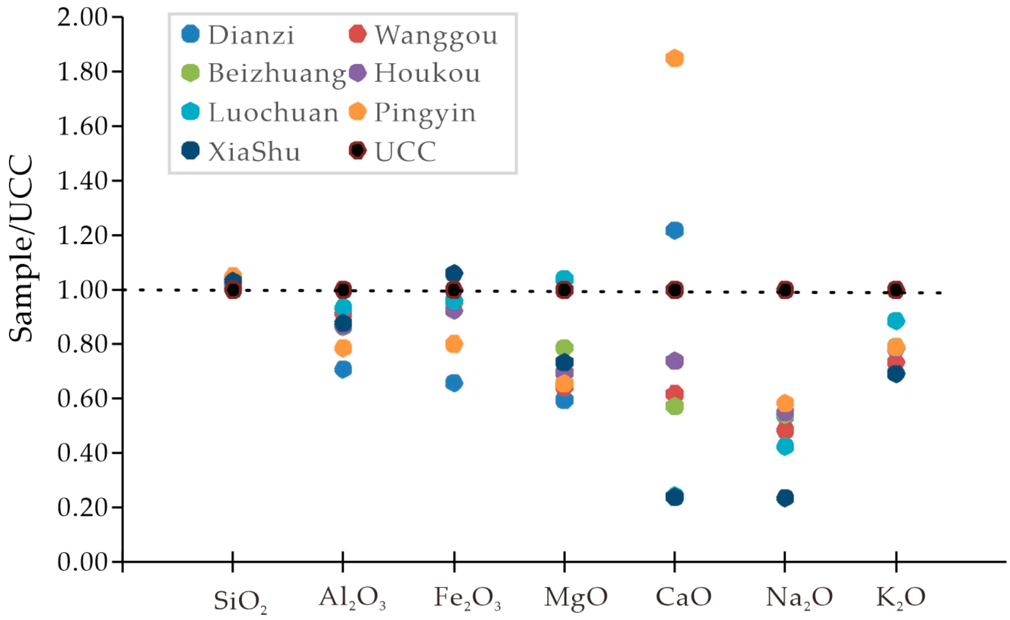

Figure 7. UCC normalized pattern of major elements of the Miaodao Islands loess and its comparison with Luochuan loess [55], Pingyin loess [56] and Xiashu loess [57].

DZ, average of 46 loess samples from Miaodao Islands, North Changshan Island, Dianzi village west section, China (on the basis of this study).

WG, average of 51 loess samples from Miaodao Islands, South Changshan Island, Southwest of Wanggou village section, China (on the basis of this study).

BZ, average of 81 loess samples from Miaodao Islands, Daheishan Island, Beizhuang village section, China (on the basis of this study).

HK, average of 78 loess samples from Miaodao Islands, Tuoji Island, Houkou village south section, China (on the basis of this study).

LC, average of 20 loess samples from Nanking, Luochuan, Xining, Xifeng and Jixian sections, China [58–60].

XS, average of 54 loess samples from Jiangsu province, Zhenjiang city, XiaShu sections, China [57].

PY, average of 70 loess samples from Shandong province, Jinan city, Pingyin section, China [56,61].

CLP, average of seven loess samples from the Loess Plateau along a north–south transect, China [62].

GAL, Global average loess composition from the mean of seventeen (1–17) averages of eleven loess regions (n = 244) [14].

Chemical Index of Alteration (CIA) can indicate the degree of chemical weathering of feldspars into clay minerals [63,64]. CIA is defined as $Al_2O_3/(Al_2O_3 + CaO^* + Na_2O + K_2O) \times 100$ (molar contents, with CaO* being CaO content in silicate fraction of the sample) [65]. Our correction procedure for CaO* follows that in [66]: (1) CaO is first corrected for that residing in apatite using P_2O_5 data ($CaO' = CaO - 10/3 \times P_2O_5$), and (2) if CaO′ is greater than Na_2O, the final CaO* value is set equal to Na_2O, but if CaO′ is less than Na_2O, the final CaO* is set equal to CaO′ [67]. Kaolinite has a CIA value of 100 and represents the highest degree of weathering. Intermediate weathering products yield somewhat lower CIA values, e.g., illite 75–90 and muscovite 75, and primary minerals and rocks yet lower values, e.g., feldspars 50, fresh granites and granodiorites 45–55, and fresh basalts 30–45 [63,65]. The Na/K ratio reflects silicate weathering intensity (plagioclase vs. K-feldspars). Therefore, the ratio of Na/K reflects the degree of cementation in supergene action and can be used to reflect the degree of loess soil formation. It is an index to measure the degree of plagioclase weathering in the sample [34,68,69].

The CIA and Na/K calculation results (Figure 8) show that the loess on the Miaodao Islands has experienced incipient chemical weathering (50–65), and a small amount has fallen into intermediate chemical weathering (65–70), indicating that plagioclase has undergone a certain degree of weathering. The degree of weathering of potassium feldspar is low, which is consistent with published results from the Miaodao loess [40]. It is generally revealed that the weathering after loess deposition has a limited impact on the overall change of sediment particle size and mineral composition [70].

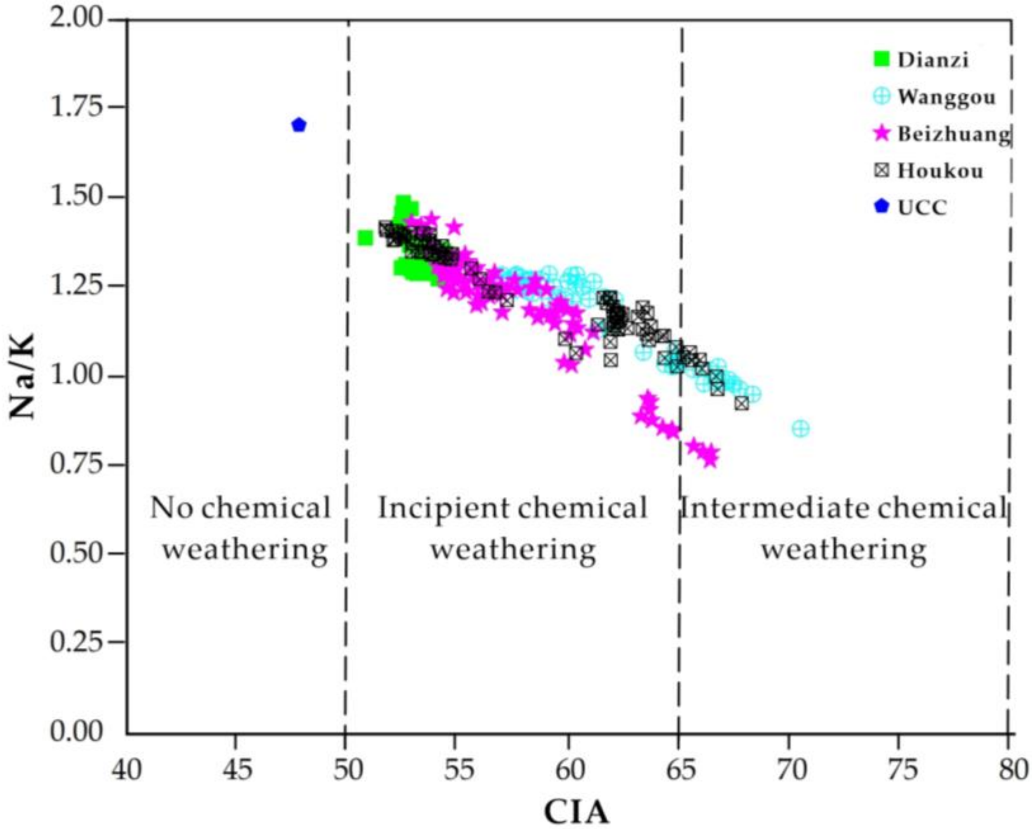

Figure 8. The scatter diagram of CIA and Na/K molar ratio of the Miaodao Islands loess.

Nesbitt et al. (1982) proposed the A-CN-K (Al_2O_3-CaO^* + Na_2O-K_2O) triangular model diagram of continental weathering to reflect the chemical weathering trend of profile strata. CaO* is the molar content of silicate minerals. The basic principle is that terrigenous shale is the primary weathering product of typical upper continental crust (UCC), and the direction of UCC pointing to terrigenous shale represents the typical early continental weathering trend [63]. The A-CN-K diagram (Figure 9) show that the weathering trend of loess sections in Miaodao Islands is consistent with that of continental weathering, but these sediments are in different weathering stages, which indicates that the loess dust material in Miaodao Islands also originates from the extensive upper continental crust and is highly mixed in the process of wind transport and deposition. The loess data points are basically parallel to the A-CN join, indicating that the plagioclase in the profile has been weathered and decomposed, Ca and Na leached and migrated, while the potassium feldspars remained relatively stable. Compared with other typical eolian deposits, the loess of Miaodao Islands is closer to terrestrial shale and Luochuan loess, and farther away from UCC, indicating that its chemical weathering intensity is in the incipient chemical weathering stage (Ca and Na removal).

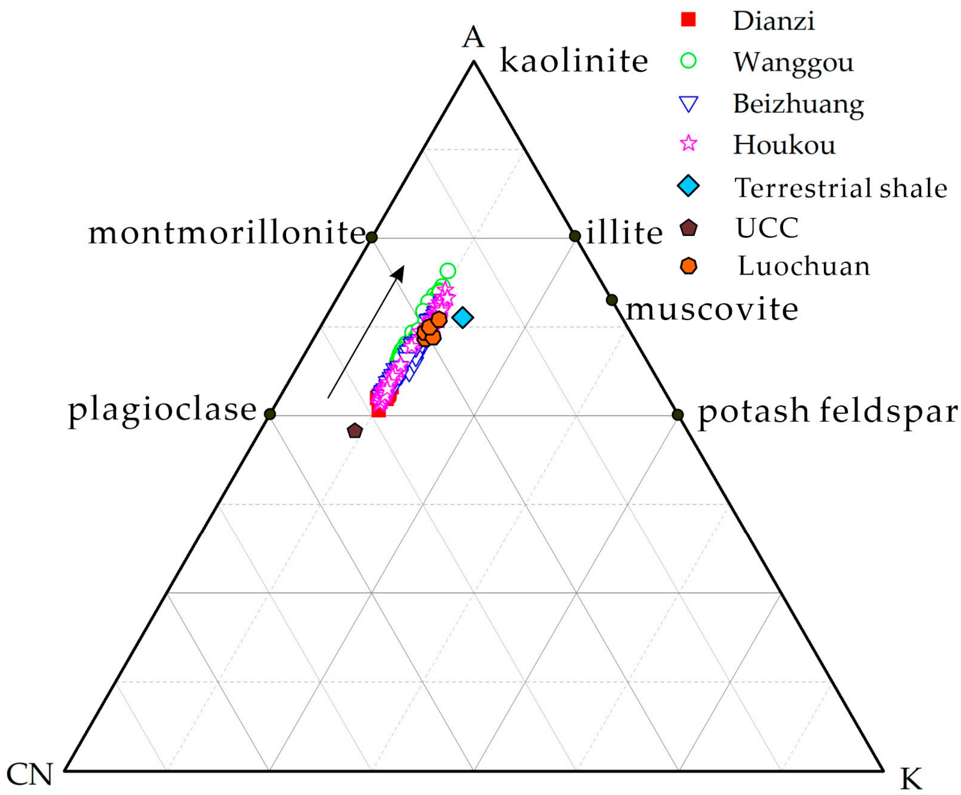

Figure 9. A-CN-K diagram of Miaodao Islands loess (Arrows represent continental chemical weathering trends, A for Al_2O_3, CN for $CaO^* + Na_2O$, K for K_2O, terrestrial shale for Post-Archean Australian Shale (PAAS)).

The composition of loess is complex, and important information regarding its provenance can be obtained by comparing the geochemical characteristics of loess with those of common rock constants elements. The two methods have high sensitivity and good effect for analysis of loess's provenance [51,71]. The first method considers the three most important sedimentary rock geochemical characteristics, namely shale (shale metamorphosed from slate), carbonate (limestone and dolomite), and sandstone, in addition to igneous rocks that vary continuously from felsic to mafic. The horizontal axis $\mathrm{Log}[(CaO + Na_2O)/K_2O]$ is used to distinguish the ratio of carbonate to plagioclase and potassium feldspar, while the vertical axis Log (SiO_2/Al_2O_3) is used to distinguish the ratio of quartz to feldspar and clay minerals. From Figure 10, it can be seen that the loess of the Miaodao Islands and the loess of the Loess Plateau are both distributed at the contact between sandstone and shale, which is due to the fact that loess is mainly composed of silt, and the particle size is between sandstone and shale. The $\mathrm{Log}[(CaO + Na_2O)/K_2O]$ value of the Miaodao Islands loess is mostly smaller than that of the Loess Plateau loess, indicating that the proportion of carbonate and plagioclase to potassium feldspar is relatively small, while the proportion of potassium feldspar is larger. From its relationship with igneous rocks, the Loess Plateau loess is close to the average value of igneous rocks, while the Miaodao Islands loess is closer to the position of granite, indicating that the provenance of the Loess Plateau loess is mainly the average composition of the upper continental crust (granodioritic in composition), while the Miaodao Islands loess is closer to a granitic composition.

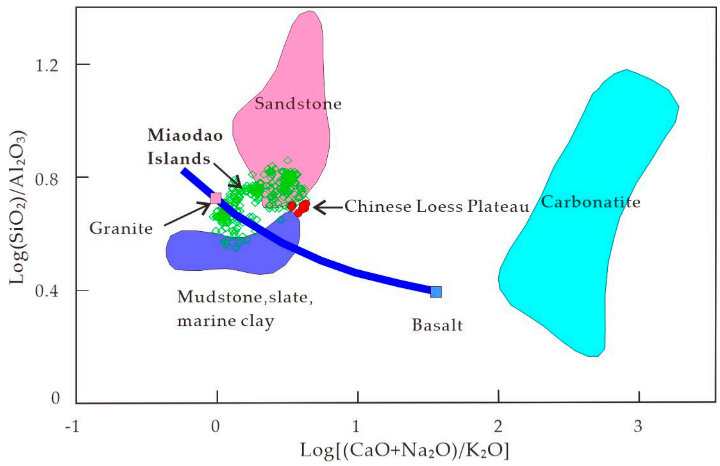

Figure 10. Plot of major element ratios used for geochemical classification of sedimentary rocks and comparison of loess compositions with the Miaodao Islands defined by these rocks. Data sources: Chinese Loess Plateau [59,60,62].

The second method of distinguishing the relative contributions of acidic igneous rocks (granite and rhyolite) and basic igneous rocks (basalt and diabase) to loess is by comparing K_2O/Al_2O_3 with Na_2O/Al_2O_3 [71]. The vertical axis of Na_2O/Al_2O_3 can be used to distinguish the ratio of igneous rocks to sedimentary rocks, while the horizontal axis of K_2O/Al_2O_3 can be used to distinguish the felsic/mafic nature of igneous rocks. The shale trend line is derived empirically, indicating sedimentary rocks or metamorphic rocks with low Na_2O and high Al_2O_3, including shale, slate, mudstone, schist, and phyllite. The shale trend line is lower than the igneous rock region because sedimentary rocks and other clastic rocks have undergone chemical weathering of plagioclase, resulting in lower Na_2O than igneous rocks. As shown in Figure 11, the loess in Harbin, Northeast China [72], the loess in the Chinese Loess Plateau [59], and the loess in the Qinling Mountains [47] are distributed in three distinct regions, while the loess on the Miaodao Islands is distributed in all three regions, indicating that the loess on the Miaodao Islands is derived from a complex source, i.e., both fine-grained sedimentary or metamorphic rocks and intermediate-acidic igneous rocks.

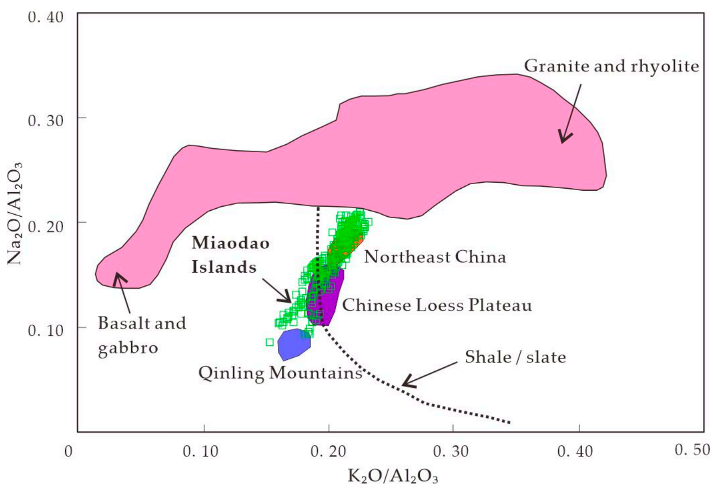

Figure 11. Plot of major element ratios used for comparison of sedimentary rock compositions to field of igneous rock compositions and shale compositional trend line. Data sources: Chinese Loess Plateau [59,60,62]; Northeast China [72]; Qinling Mountains [73].

3.2. Trace Elements

The characteristics of relatively rich Zr in the loess of the Miaodao Islands indicate that the loess of the Miaodao Islands comes from near source materials with coarser particle sizes, which is consistent with the coarser particle size of the loess on the Miaodao area. As shown in Figure 12, the trace element curves of the Miaodao Islands profiles are generally similar, although there are certain differences between them. Specifically, V, Cr, Cs, Ni and Li are completely enriched relative to the upper crust, Sr, U, Nb, Ta, Be, Cu, Mo, Cd, Sn, Sc, and Tl are depleted, and the remaining elements are similar to or partially depleted and partially enriched relative to the upper crust. The trace elements commonly used to determine the source of sedimentary rocks are mostly immobile elements in the near surface and low temperature environment, such as Cr, Sc, Ta, Th, Zr, Hf, and Y. The Sc-Th-La triangular diagram is a commonly used method for distinguishing sources. Sc is mainly enriched in pyroxene, and Th and La are enriched in granite, so sedimentary rocks originating from basic rocks are close to Sc, and those originating from granitic rocks are located between Th and La. As shown in Figure 13 (left), the loess of the Miaodao Islands and the CLP [74] are both located in the upper part of the continental margin arc, and the two have obvious overlap, indicating that the two sources are felsic rocks. The loess of the Tibetan Plateau [74] shows a higher enrichment of La and Th, indicating that its source has a higher felsic component. The Zr-Sc-Th triangular diagram is another commonly used tool for distinguishing sources. As shown in Figure 13 (right), the loess of the Miaodao Islands and the Loess Plateau are located in the same area, indicating that the two sources are the same, both from felsic rocks. The loess of the Tibetan Plateau has a higher content of Zr and Th, indicating that its source has a higher felsic component, while the loess of Tajikistan [75] has a higher Sc content, indicating that its loess source is more basic.

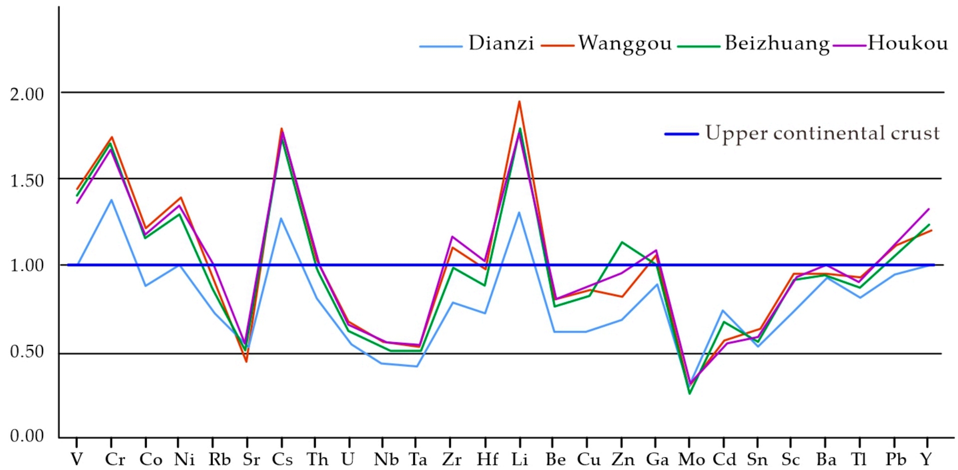

Figure 12. The Upper Continent Crust-normalized plot of trace element concentrations of Miaodao Islands loess.

The elements Th and Zr are enriched in felsic rather than in mafic rocks because they are highly incompatible during most igneous melting and fractionation processes [76,77]. The Zr/V and Zr/Ni ratios are useful proxies of zircon enrichment since Zr is enriched in zircon, whereas V and Ni generally preserves a signature of the provenance. At the same time, Th/V and Th/Ni are good overall indicators of igneous chemical differentiation processes since Th is incompatible, whereas V and Ni are typically compatible elements in igneous systems [66]. Thus, heavy mineral (e.g., zircon, monazite) enrichment due to sedimentary sorting and recycling has been tested using Zr/V vs. Th/V, and Zr/Ni vs. Th/Ni diagrams (see [14]). The possibility of heavy mineral enrichment was tested using Th/V vs. Zr/V, and Th/Ni vs. Zr/Ni ratios (Figure 14a,b), which in addition to Cr/V and Y/Ni ratios are good overall indicators of igneous chemical differentiation processes [14,76–78]. Additionally, compatible trace elements, such as Cr, are useful in identifying accessory detrital components such as chromite, commonly derived from mafic to ultramafic sources including ophiolites, not readily recognized by petrography alone [14,15,79]. The Th/V vs. Zr/V and Th/ Ni vs. Zr/Ni data are above both the primary compositional trend (Figure 14a,b; dashed line with arrow) defined by igneous rocks at high Zr/metal ratio [80] and the average value of UCC and PAAS. The elements Th and Zr are enriched in felsic rather than in mafic rocks because they are highly incompatible during most igneous melting and fractionation processes [76,77]. High Zr/metal ratios clearly demonstrate zircon enrichment in loess samples of Miaodao islands compared to UCC, PAAS sediments, implying that aeolian (or combined fluvialaeolian) transport efficiently concentrates zircon minerals [15,77]. High Zr/V and Zr/Ni ratios suggested zircon enrichment in these sediments, which is an indication of well-mixed and recycled dust source. This also supported by the fact that our data plotted close to Table 2, Supplementary Table S1 (BZ, DZ, HK, WG) composition in a very defined region (Figure 14a,b). Th/metal vs. Zr/metal diagrams (Figure 14a,b) suggest that the source material of these Pleistocene and Holocene sediments must have been at least partially recycled and well homogenized during fluvial and subsequent eolian transports. The above interpretation was additionally supported by TiO_2 vs. Ni [81] and Cr/V vs. Y/Ni provenance diagrams [14,66] (Figure 14c–d). The loess sample values corresponded to the composition of acidic rocks as plotted close to Table 2, Supplementary Table S1 (BZ, DZ, HK, WG). Lower Ni content and higher Y/Ni ratios were detected in the loesses than in the UCC and PAAS. Nickel is positively correlated with TiO_2 (Figure 14c), suggesting that it might be bound in Ti-bearing phyllosilicates. Nevertheless, the general depletion of compatible elements, such as Cr, V, and Ni (Figure 14c), supported the fact that the amounts of mafic or ultramafic rocks were insignificant in the source area [14,76,81]. In the Ni vs. TiO_2 space (Figure 14c), loess samples cluster at the upper margin of the field of acidic rocks and plot close to GAL. The TiO_2 values of the Paks sediments are generally higher than those in most acidic rocks, while the Ni values are well within the range characteristic for acidic rocks. The higher TiO_2 values can be explained by Ti-bearing heavy mineral enrichment (e.g., rutile, titanite) resulting from sedimentary sorting and recycling. Higher Y/Ni and similar Cr/V ratios were found in the loesses from Miaodao islands compared to the UCC (Figure 14d). Since mafic rocks have high ferromagnesian trace element abundances (low Y/Ni and high Cr/V in ultramafic rocks) and lower abundances of compatible elements such as Cr, V and Ni in the Paks sediments were found, a contribution from mafic/ultramafic sources to the Miaodao islands sediments seems to be insignificant (Figure 14c,d). At the same time, these provenance diagrams suggest that sediments in the Miaodao islands section may have the similar source as the CLP. This observation is consistent with previous findings of [9,12,22,82].

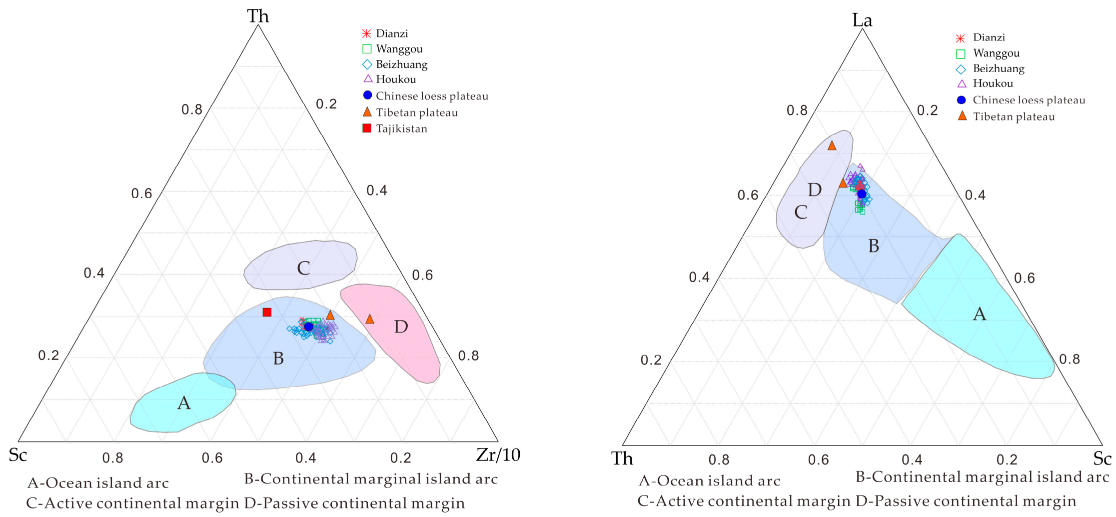

Figure 13. Sc-Th-La and Zr-Sc-Th plots of Miaodao Islands loess.

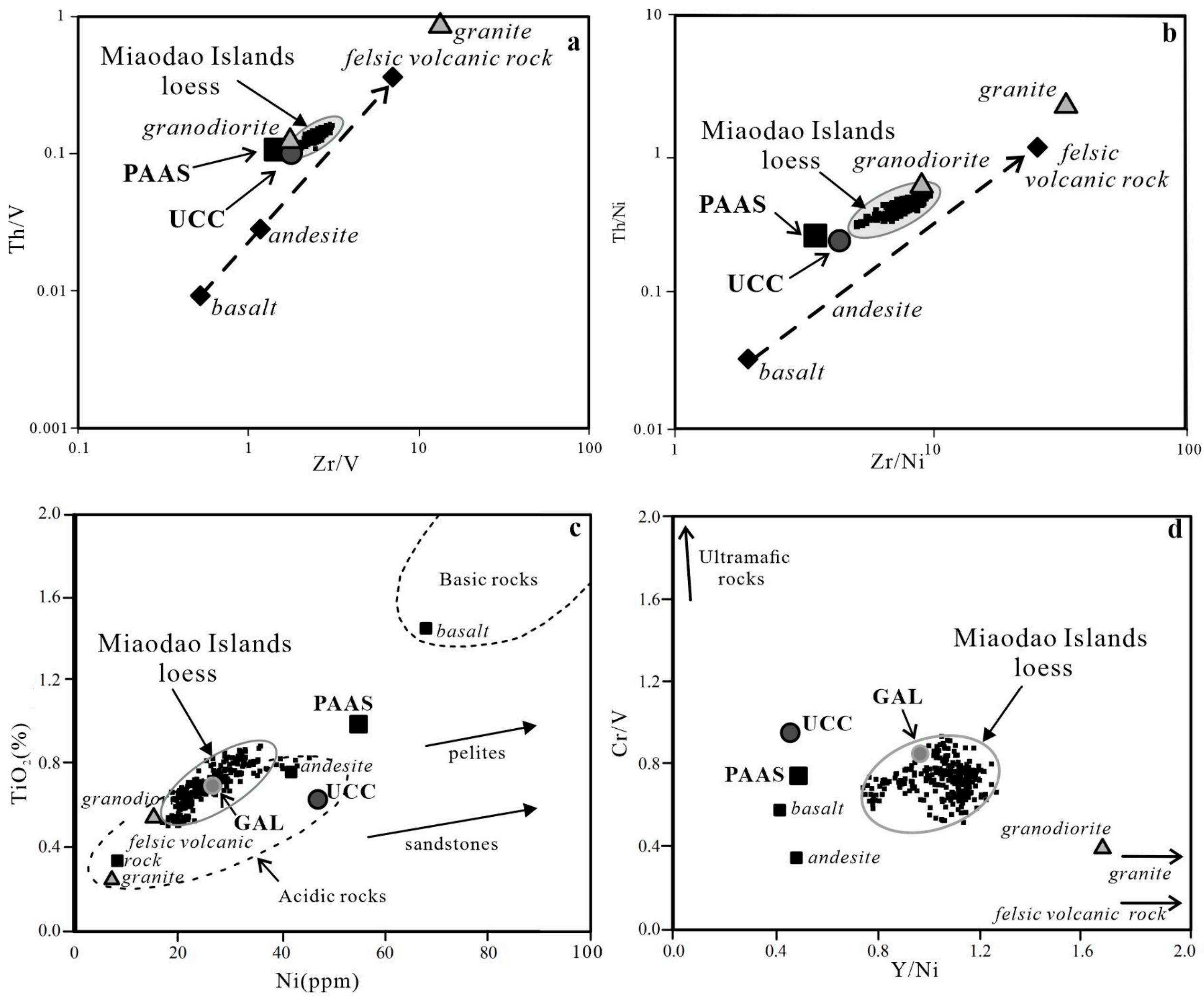

Figure 14. Plots of (**a**) Zr/V vs. Th/V, (**b**) Zr/Ni vs. Th/Ni, and provenance discrimination diagrams of (**c**) Ni vs. TiO_2 [81] and (**d**) Y/Ni vs. Cr/V ([83]) for comparing loess and paleosol samples from the Miaodao islands loess section and global average loess composition (GAL; [14]), post-Archean Australian average shale (PAAS; [76,77];), and Upper Continental Crust (UCC; [84]). Igneous rock compositions on a) and (**b**) are average values from [80]. In panel (**d**), the samples were also compared to ultramafic rock (UMF) and granite (GRN) compositions ([78]).

3.3. Rare Earth Elements

REEs are highly immobile in near-surface environments and are hosted formed in a variety of minerals, thus loess REE compositions can represent both proximal and distal sedimentary sources. In order to eliminate the influence of the odd-even effect of rare earth elements, the average value of rare earth elements in chondrite was used as the standard, and the rare earth element values of the samples were standardized to study the distribution pattern of rare earth elements. The normalized value of rare earth elements chondrite is the ratio of the amount of each rare earth element in the sample to the amount of each rare earth element corresponding to the chondrite. Since the chondrite has been recognized as the original material of the earth, the rare earth elements in it have not been fractionated. Therefore, the rare earth elements in the sample can be clearly seen after the standard mapping. Fractionation characteristics of soil elements. The specific method is: the ratio of the rare earth element content of the sample to the rare earth element content in the chondrite is used as the ordinate, and the La-Lu is arranged according to the atomic number as the abscissa, that is, the standardized rare earth element distribution curve of the chondrite is obtained. As shown in Figure 15, both the Miaodao Islands loess and the Luochuan loess of the Loess Plateau show the common characteristics of LREE enrichment, small negative Eu anomaly, and relatively flat HREE. The REE distribution curves of each section of the Miaodao Islands loess are extremely similar, indicating that the source material of the loess is the same. The europium (Eu) anomaly is the phenomenon whereby the europium (Eu) concentration in a mineral is either enriched or depleted relative to some standard, commonly a chondrite or mid-ocean ridge basalt (MORB). In geochemistry a europium anomaly is said to be "positive" if the Eu concentration in the mineral is enriched relative to the other REEs, and is said to be "negative" if Eu is depleted relative to the other REEs. Rare earth element concentrations have been normalized to chondrite from [85]. Eu anomalies (Eu/Eu*) have been calculated as $Eu/Eu^* = Eu_N/(Sm_N \times Gd_N)^{0.5}$; the subscript $_N$ shows that the value was normalized by the chondrite [86]. Eu/Eu* can indicate the ultimate source of sediment, usually Eu/Eu* = 1 for mantle source, >1 for lower crustal source, and <1 for upper crustal source, with values of loess mostly between 0.6–1. The average Eu/Eu* values of the Miaodao Islands loess range from 0.65 to 0.69, and the Luochuan loess is slightly lower at 0.63, with an average upper crustal value of 0.65. ΣLREE/ΣHREE indicates the degree of light and heavy rare earth element fractionation, with average values of the Miaodao Islands loess ranging from 7.84 to 8.31, and the Luochuan loess at 11.67, with an average upper crust value of 13.51. La_N/Yb_N (ratio of rare earth elements La and Yb, the subscript $_N$ shows that the value was normalized by the chondrite) indicates the enrichment degree of light rare earth elements, with average values of the Miaodao Islands loess ranging from 8.02 to 9.99, and the Luochuan loess at 7.93, with an average upper crust value of 9.19. Gd_N/Yb_N indicates the degree of heavy rare earth element depletion, with average values of the Miaodao Islands loess ranging from 1.40 to 1.76, and the Luochuan loess at 1.53, with an average upper crust value of 1.39 (Table 4). As shown in Figure 15, both the Miao Islands loess and the Luochuan loess of the Loess Plateau show the common characteristics of LREE enrichment, small negative Eu anomaly, and relatively flat HREE. The REE distribution curves of each section of the Miao Islands loess are extremely similar, indicating that the source material of the loess is the same.

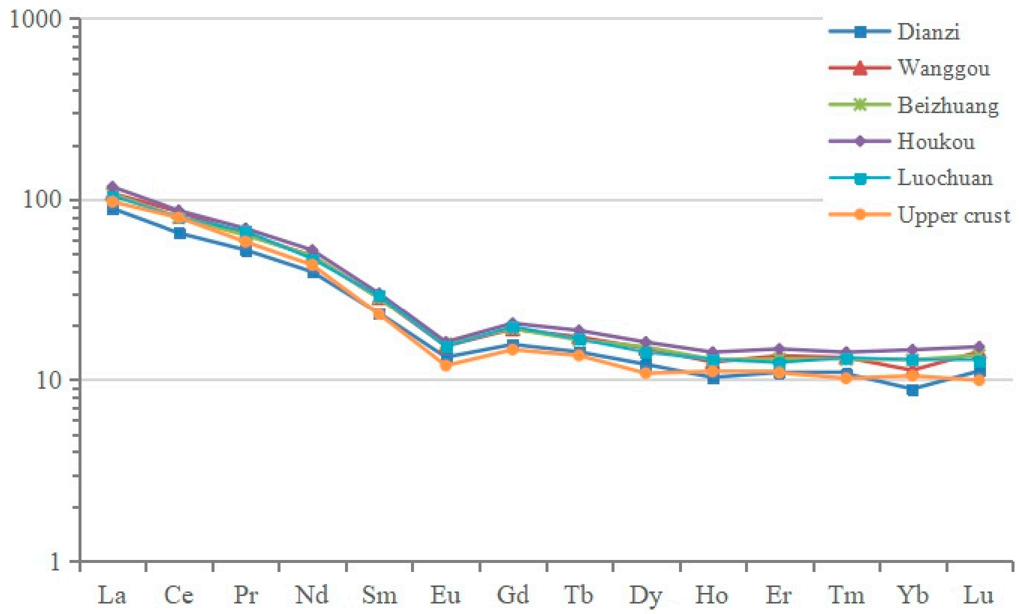

Figure 15. Chondrite-normalized plots of REE concentrations.

Table 4. REE concentrations and values concerned of Miaodao Islands loess.

Location	Sample Quantity	Element	La	Ce	Pr	Nd	Sm	Eu	Gd	Data Sources
Dianzi	46	mean value	27.57	52.56	6.40	23.83	4.56	0.98	4.06	This test
		element	Tb	Dy	Ho	Er	Tm	Yb	Lu	
		mean value	0.67	3.92	0.74	2.31	0.35	1.86	0.36	
		ΣREE	130.19	ΣLREE	115.92	ΣHREE	14.27	ΣLREE/ΣHREE	8.12	
		Eu/Eu*	0.69	La_N/Yb_N	9.99	Gd_N/Yb_N	1.76			
Wanggou	51	element	La	Ce	Pr	Nd	Sm	Eu	Gd	
		mean value	33.37	68.85	7.81	29.19	5.55	1.13	4.94	
		Element	Tb	Dy	Ho	Er	Tm	Yb	Lu	
		mean value	0.81	4.81	0.90	2.85	0.43	2.36	0.46	
		ΣREE	163.47	ΣLREE	145.92	ΣHREE	17.55	ΣLREE/ΣHREE	8.31	
		Eu/Eu*	0.66	La_N/Yb_N	9.57	Gd_N/Yb_N	1.69			
Beizhuang	81	element	La	Ce	Pr	Nd	Sm	Eu	Gd	
		mean value	33.15	63.88	7.73	29.20	5.55	1.16	4.98	
		element	Tb	Dy	Ho	Er	Tm	Yb	Lu	
		mean value	0.78	4.89	0.93	2.74	0.42	2.69	0.44	
		ΣREE	158.55	ΣLREE	140.67	ΣHREE	17.88	ΣLREE/ΣHREE	7.87	
		Eu/Eu*	0.68	La_N/Yb_N	8.32	Gd_N/Yb_N	1.49			
Houkou	78	Element	La	Ce	Pr	Nd	Sm	Eu	Gd	
		mean value	36.29	69.95	8.41	31.42	5.88	1.19	5.32	
		Element	Tb	Dy	Ho	Er	Tm	Yb	Lu	
		mean value	0.88	5.20	1.02	3.11	0.46	3.06	0.49	
		ΣREE	172.68	ΣLREE	153.15	ΣHREE	19.54	ΣLREE/ΣHREE	7.84	
		Eu/Eu*	0.65	La_N/Yb_N	8.02	Gd_N/Yb_N	1.40			
Luochuan	7	element	La	Ce	Pr	Nd	Sm	Eu	Gd	[59]
		mean value	32.3	64.6	8.16	28.1	5.70	1.12	5.11	
		element	Tb	Dy	Ho	Er	Tm	Yb	Lu	
		mean value	0.79	4.57	0.93	2.61	0.43	2.70	0.41	
		ΣREE	157.54	ΣLREE	145.11	ΣHREE	12.43	ΣLREE/ΣHREE	11.67	
		Eu/Eu*	0.63	La_N/Yb_N	7.93	Gd_N/Yb_N	1.53			
Upper crust		element	La	Ce	Pr	Nd	Sm	Eu	Gd	[76]
		mean value	30	64	7.1	26	4.5	0.88	3.8	
		element	Tb	Dy	Ho	Er	Tm	Yb	Lu	
		mean value	0.64	3.5	0.80	2.3	0.33	2.2	0.32	
		ΣREE	146.37	ΣLREE	136.28	ΣHREE	10.09	ΣLREE/ΣHREE	13.51	
		Eu/Eu*	0.65	La_N/Yb_N	9.19	Gd_N/Yb_N	1.39			

Note: Eu/Eu*, Eu is chondrite normalized value, Eu* = $(Sm_N \times Gd_N)^{0.5}$.

In recent years, La_N/Yb_N-Eu/Eu* diagrams have become an effective means of distinguishing the source of loess. As shown in Figure 16, the numerical values of Miaodao Islands loess fall in the transition zone between the Qilian Mountains rocks, Altai Mountains and Mongolian Gobi rocks, and the loess of the CLP, with most of them falling within the range of the CLP, indicating that may share common sources. Sun [22,82] used this method to compare the loess of the Qaidam Basin, Tarim Basin and Junggar Basin with the loess of the CLP, revealing that although the loess of the Loess Plateau overlaps with the data of the Qaidam Basin and Tarim Basin, most of them fall outside the range of the two, and there is no overlap with the data of the Junggar Basin, with most of the data falling in the transition zone between the Qilian Mountains and Altai Mountains and Mongolian Gobi rocks. From the above facts, we infer that the loess of Miaodao Islands and the loess of the Loess Plateau both come from the alluvial fan deposits of the Qilian Mountains, Mongolian Gobi-Altai Mountains and Hangai Mountains.

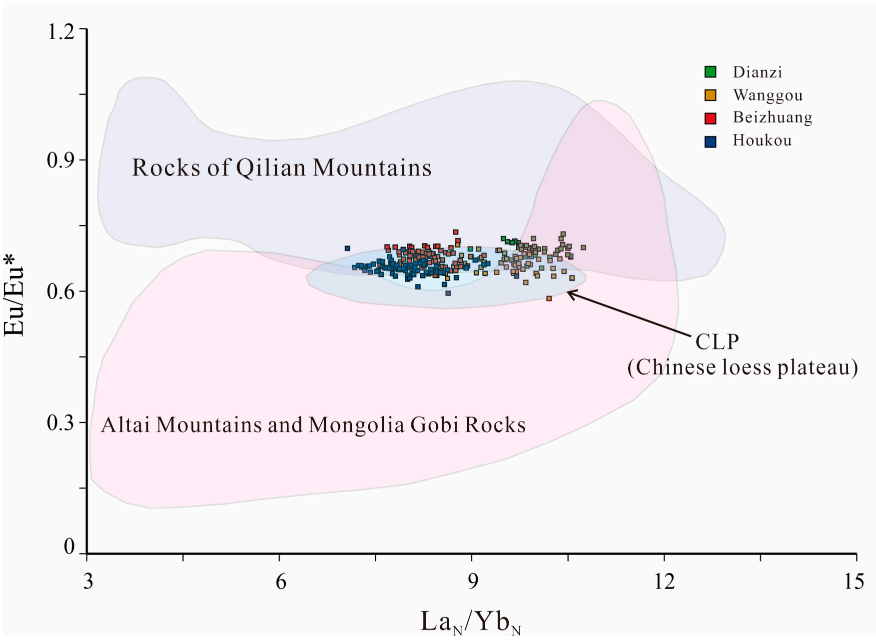

Figure 16. The La_N/Yb_N versus Eu/Eu* plot of Miaodao Islands loess (Chinese Loess Plateau La_N/Yb_N and Eu/Eu* data are from [59,60,62,74,82]; ranges of La_N/Yb_N and Eu/Eu* values for the Qilian Shan, Altay Mountains, and Mongolian Gobi are from compilation by [87] and sources therein, Range of compositions of rocks from the Qilian Shan (see [51]'s Figure 2 and Figure 23b for location) and the Altay Mountains and Mongolian Gobi (see [51] Figure 2 for location).

4. Conclusions

(1) Through the geochemical analysis of major and trace elements in four typical loess profiles of Dianzi in North Changshan island, Wanggou in South Changshan island, Beizhuang in Daheishan island and Houkou in Tuoji island, it can be seen that the variation of major and trace elements in the loess of Miaodao Islands is relatively restricted, which reflects that the loess deposits of in Miaodao Islands have the same provenance and formation mechanism. From the change curve of major elements (Figure 6), except that CaO may be greatly changed by syndepositional weathering and leaching, the other change curves (Figure 6) fluctuate a little. The CIA and Na/K calculation indicated that the loess on the Miaodao Islands had experienced incipient chemical weathering. The A-CN-K diagram showed that the loess dust material on the Miaodao Islands originated from the extensive upper continental crust and was highly mixed in the process of wind transport and deposition. High SiO_2 shows a high degree of provenance sorting. $Log[(CaO + Na_2O)/K_2O] - Log(SiO_2/Al_2O_3)$ and Na_2O/Al_2O_3-K_2O/Al_2O_3 diagrams show that compared with the loess of the CLP, the loess of the Miaodao Islands contains more granite components, and its provenance is more complex than the CLP loess, that is, it may be derived from fine-grained sedimentary rocks or metamorphic rocks, and from intermediate-acidic igneous rocks. The immobile trace elements in the near-surface and low-temperature environment play a significant role in tracing the provenance. The variation of REE element distributions of Miaodao Islands loess is very similar to that of Luochuan and upper continental crust, showing the common characteristics of LREE enrichment, small Eu negative anomaly and relatively flat HREE. From the L_aN/Y_bN − Eu/Eu* diagram, it can be seen that the vast majority of the loess on the Miaodao Islands falls within the variation range of the CLP loess, and the rock of the Qilian Mountains and the Altai Mountains and Mongolia Gobi rock junction. The source discrimination diagrams of Sc-Th-La and Zr-Sc-Th show that the loess of the Miaodao Islands is similar to the CLP loess, but is significantly different from the loess of the Qinghai-Tibet Plateau and Tajikistan further to the west. All of these indicate that the loess of the Miaodao Islands and the CLP loess may have a common source, which includes

the alluvial fan deposits of the Qilian Mountains, Mongolian Gobi-Altai Mountains and Hangai Mountains in the northwest.

(2) There are also many contradictions between the loess of the Miaodao Islands and the sedimentary material transported from a distant source. Firstly, the average SiO_2 content of the loess of the Miaodao Islands is 67–69%, which is higher than the average value of Luochuan and the upper continental crust. The known mechanisms of loess transport would imply that the sand and coarse particle silt content should decrease, likewise the SiO_2 concentration with increasing source distance. Secondly, Chinese loess has the characteristics of relative enrichment of Cs, deficiency of Zr and Hf, which is related to the desert loess formed by long-distance transportation, while the loess of the Miaodao Islands is relatively enriched in Zr. This phenomenon may be related to the recycling and enrichment effect of near source sediments. Thirdly, the grain size of the loess of the Miaodao Islands is dominated by the coarse silt grain size, which is much coarser than that of Luochuan loess, and there is a decreasing trend of sand content with the geographical location from north to south [34,36,40,48]. Fourthly, the Malan loess in the upper part of the Miaodao Islands contains many marine microfossils, such as foraminifera, ostracods and radiolarians, most of which suffered shell erosion and damage, while the lower lithic loess is devoid of marine fossils [33,35]. Fifthly, there are interbedded gravel layers or gravel particles in the loess of the Miaodao Islands. All these facts indicate that the loess of the Miaodao Islands has an allochthonous near-source feature.

(3) The ages of the OSL samples at the depths of 1.0 m~7.0 m are 11.8 $\pm$ 1.4 ka ~67.7 $\pm$ 1.2 ka (Figure 3), indicating that the aeolian sediments were deposited after the Late Pleistocene. The loess profiles recorded the paleoclimatic changes in this region since the last interglacial period. There are significant differences in the sedimentation rate of loess on Miaodao Islands in different periods. The loess layer corresponds to periods of dry and cold climate, while the paleosol layer corresponds to periods of warm and humid climate, which was conducive to pedogenesis. In summary, the loess profiles reveal cyclical changes of climate in the eastern coastal area of China since the last glacial period [40]. The loess of Miaodao Islands is mainly deposited during low sea level periods, but when sea level rises, the sedimentation rate slows down, and even the strata are missing [10]. In addition, under the background of the impact of sea level change, loess accumulation in different areas of Miaodao Islands also has some differences in thickness and stratum.

(4) Based on the above analysis and OSL dating data by integrating previously published data from the literature, we conclude that during the Middle Pleistocene Loess deposition period, the material of the Miaodao Islands Loess may have originated mainly from distant sources, with a very small amount of gravel and debris from local sources. Since the Late Pleistocene, with the development of glacier action and the decrease of sea level, the bottom of the Bohai Sea was gradually exposed, and the shallow sea sediments, river-lake sediments, and slope-flood sediments originally deposited in the Bohai Sea Basin became near-source materials, which together with distant-source materials constituted the sources of the Miaodao Islands Loess. With the repeated sea level retreats of the Bohai Sea, during the last glacial period, the bottom of the Bohai Sea was completely exposed, and the seabed sediments became the main source of the Miaodao Islands Loess, while the distant-source sediments became secondary (Figure 17). Therefore, the Miaodao Islands loess contains both near- and far- source materials, and the source of the materials has changed with the changes of sea level and paleoenvironmental change.

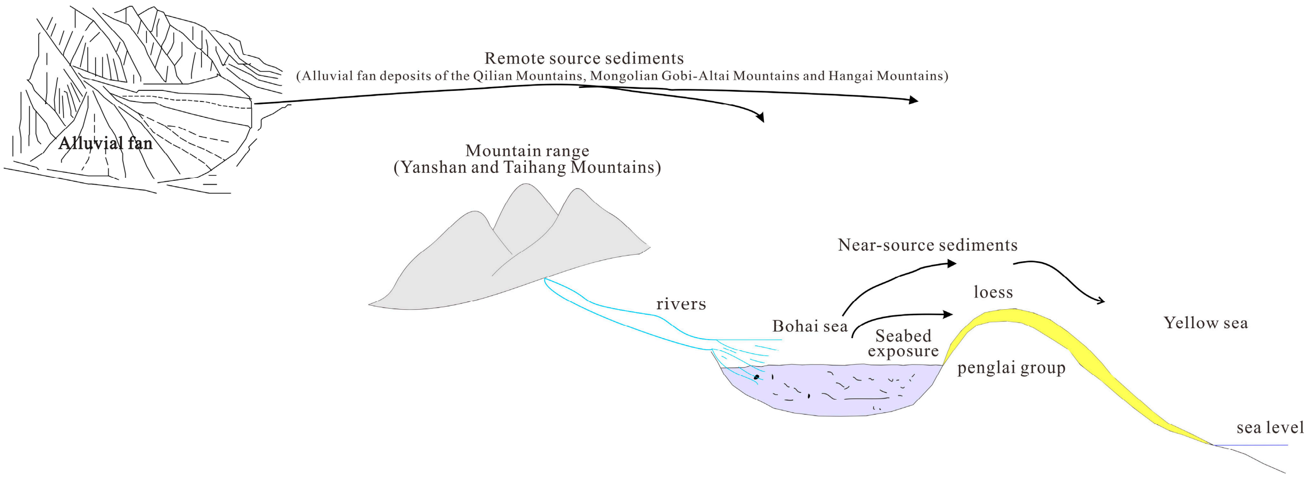

Figure 17. Schematic representation of the loess formation on the Miaodao Islands during the Last Ice Age.

Supplementary Materials: The following supporting information can be downloaded at: https://www.mdpi.com/article/10.3390/atmos15030261/s1; Table S1: Geochemical elements test data on the Miaodao Islands.

Author Contributions: Conceptualization, K.W., J.S. and Y.Z.; methodology, K.W. and P.L.; software, J.S.; validation, K.W. and X.Q.; formal analysis, K.W.; investigation, Y.X., M.L., K.G. and L.W.; data curation, C.X.; writing—original draft preparation, J.S.; writing—review and editing, K.W., P.L. and M.R.; visualization, K.W. All authors have read and agreed to the published version of the manuscript.

Funding: This research was funded by the Study Abroad Programme of Shandong Provincial Government (201902006), Shandong Engineering Research Center for Environmental Protection and Remediation on Groundwater Open Foundation (801KF202006), State Key Laboratory of Loess and Quaternary Geology Open Foundation (SKLLQJ2114), Shandong Geological Exploration Fund (202208), Key Laboratory of Coastal Science and Integrated Management, Ministry of Natural Resources Open fund (2021COSIMQ006), Science and Technology Innovation Cultivation Plan Project of Institute of Shandong Geological Sciences (PYJH202101).

Institutional Review Board Statement: Not applicable.

Informed Consent Statement: Not applicable.

Data Availability Statement: The data presented in this study are available on request from the corresponding author. The data are not publicly available due to privacy.

Acknowledgments: Many thanks to Jingxiang Tian and Wei Zhao for their administrative and laboratory assistance. We are grateful for critical comments and suggestions by the reviewers.

Conflicts of Interest: The authors declare no conflicts of interests.

References

1. Pécsi, M. Loess is not just the accumulation of dust. *Quat. Int.* **1990**, *7–8*, 1–21. [CrossRef]
2. Li, Y.D.; Li, Y.; Song, Y.G.; Wei, H.; Wang, Y.; Shukurov, N. Effective Moisture Evolution since the Last Glacial Maximum Revealed by a Loess Record from the Westerlies-Dominated Ili Basin, NW China. *Atmosphere* **2022**, *13*, 1931. [CrossRef]
3. Li, Y.R.; Shi, W.H.; Aydin, A.; Beroya-Eitner, M.A.; Gao, G. Loess genesis and worldwide distribution. *Earth-Sci. Rev.* **2020**, *201*, 102947. [CrossRef]
4. Li, Y.; Gholami, H.; Song, Y.; Fathabadi, A.; Malakooti, H.; Collins, A.L. Source fingerprinting loess deposits in Central Asia using elemental geochemistry with Bayesian and GLUE models. *Catena* **2020**, *194*, 104808. [CrossRef]
5. Liu, T.S. *Loess and Environment*; Science Press: Beijing, China, 1985; pp. 1–475.
6. Muhs, D.R.; Bettis, E.A.; Chan, M.A. Quaternary loess-Paleosol sequences as examples of climate-driven sedimentary extremes. *Spec. Pap. (Geol. Soc. Am.)* **2003**, *370*, 53–74. [CrossRef]
7. Song, Y.G.; Chen, X.L.; Qian, L.B.; Li, C.; Li, Y.; Li, X.; Chang, H.; An, Z. Distribution and composition of loess sediments in the Ili Basin, Central Asia. *Quat. Int.* **2014**, *334–335*, 61–73. [CrossRef]

8. Sun, J.; Guo, F.; Wu, H.; Yang, H.; Qiang, X.; Chu, H.; He, L.; Mei, X.; Jiang, J.; Wang, S. The sedimentary succession of the last 2.25 Myr in the Bohai Strait: Implications for the Quaternary paleoenvironmental evolution of the Bohai Sea. *Palaeogeogr. Palaeoclimatol. Palaeoecol.* **2022**, *585*, 110704. [CrossRef]
9. Wang, Y.D.; Yang, S.L.; Ding, Z.L. Provenance and paleoclimatic implications of loess deposits in Shandong Province, eastern China. *Quat. Res.* **2021**, *103*, 88–98. [CrossRef]
10. Yi, S.W.; Zeng, L.; Xu, Z.W.; Wang, Y.; Wang, X.; Wu, J.; Lu, H. Sea-level changes in the Bohai Sea, northern China, constrained by coastal loess accumulation over the past 200 ka. *Quat. Sci. Rev.* **2022**, *277*, 107368. [CrossRef]
11. Wu, P.; Xie, Y.Y.; Li, Y.; Kang, C.; Chi, Y.; Sun, L.; Wei, Z. Decoupling between circulation pattern and dust path since the last glacial in the Songnen Plain, NE China: Insights from quantitative provenance reconstruction of the Harbin dust sediments. *Aeolian Res.* **2022**, *57*, 100818. [CrossRef]
12. Yang, S.; Ding, F.; Ding, Z. Pleistocene chemical weathering history of Asian arid and semi-arid regions recorded in loess deposits of China and Tajikistan. *Geochim. Cosmochim. Acta* **2006**, *70*, 1695–1709. [CrossRef]
13. Buggle, B.; Glaser, B.; Zöller, L.; Hambach, U.; Marković, S.; Glaser, I.; Gerasimenko, N. Geochemical characterization and origin of Southeastern and Eastern European loesses (Serbia, Romania, Ukraine). *Quat. Sci. Rev.* **2008**, *27*, 1058–1075. [CrossRef]
14. Újvári, G.; Varga, A.; Balogh-Brunstad, Z. Origin, weathering, and geochemical composition of loess in southwestern Hungary. *Quat. Res.* **2008**, *69*, 421–437. [CrossRef]
15. Ujvari, G.; Varga, A.; Raucsik, B.; Kovács, J. The Paks loess-paleosol sequence; a record of chemical weathering and provenance for the last 800 ka in the mid-Carpathian Basin. *Quat. Int.* **2014**, *319*, 22–37. [CrossRef]
16. Jiang, Q.; Gao, X.; Tan, C.; Lu, H.; Peng, S.; Qiao, Y.; Hao, Q. Delayed sedimentary response of the Huanghe alluvial plain to climate change inferred from source variations of the Xiashu loess since ∼1 Ma. *Catena* **2023**, *231*, 107380. [CrossRef]
17. Liu, B.; Jin, H.; Sun, Z.; Zhao, S. Geochemical weathering of aeolian sand and its palaeoclimatic implications in the Mu Us Desert, northern China, since the Late Holocene. *J. Arid Land* **2016**, *8*, 647–659. [CrossRef]
18. Tursun, D.; Zhang, F.; Wu, F.; Liu, X.; Wu, S.; Sun, T.; Zheng, J.; Yue, J. Geochemical characterization of major elements in Gurbantunggut Desert sediments, northwestern China and their regional variations. *Aeolian Res.* **2022**, *57*, 100802. [CrossRef]
19. Hao, Q.; Guo, Z.; Qiao, Y.; Xu, B.; Oldfield, F. Geochemical evidence for the provenance of middle Pleistocene loess deposits in southern China. *Quat. Sci. Rev.* **2010**, *29*, 3317–3326. [CrossRef]
20. Pasquetti, F.; Zanchetta, G.; Bini, M.; Paffi, J.; Coltorti, M.; Lezzerini, M.; Arienzo, I.; Cremaschi, M. Potential dust sources for loess deposits in Central Italy: A geochemical case study from the Loess-Paleosol-Sequence of Ponte Crispiero (Marche). *Catena* **2023**, *226*, 107064. [CrossRef]
21. Rudnick, R.L.; Gao, S. Composition of the Continental Crust. In *Treatise on Geochemistry (Second Edition)*; Holland, H.D., Turekian, K.K., Ed.; Elsevier: Amsterdam, The Netherlands, 2014; pp. 1–51. ISBN 978-0-08-098300-4.
22. Sun, J.M. Source Regions and Formation of the Loess Sediments on the High Mountain Regions of Northwestern China. *Quaternary Res* **2002**, *58*, 341–351. [CrossRef]
23. Muhs, D.R.; Budahn, J.R. Geochemical evidence for the origin of late Quaternary loess in central Alaska. *Can. J. Earth Sci.* **2006**, *43*, 323–337. [CrossRef]
24. Qingyu, G.; Baotian, P.; Hongshan, G.; Na, L.; Hui, Z.; Junping, W. Geochemical evidence of the Chinese loess provenance during the Late Pleistocene. *Palaeogeogr. Palaeoclimatol. Palaeoecol.* **2008**, *270*, 53–58. [CrossRef]
25. Ding, J.N.; Wu, Y.Q.; Tan, L.H.; Fu, T.; Du, S.; Wen, Y.; Li, D. Trace and rare earth element evidence for the provenances of aeolian sands in the Mu Us Desert, NW China. *Aeolian Res.* **2021**, *50*, 100683. [CrossRef]
26. Han, L.; Hao, Q.Z.; Qiao, Y.S.; Wang, L.; Peng, S.; Li, N.; Gao, X.; Fu, Y.; Xu, B.; Gu, Z. Geochemical evidence for provenance diversity of loess in southern China and its implications for glacial aridification of the northern subtropical region. *Quat. Sci. Rev.* **2019**, *212*, 149–163. [CrossRef]
27. Li, G.X.; Li, P.; Liu, Y.; Qiao, L.; Ma, Y.; Xu, J.; Yang, Z. Sedimentary system response to the global sea level change in the East China Seas since the last glacial maximum. *Earth-Sci. Rev.* **2014**, *139*, 390–405. [CrossRef]
28. Li, Y.; Song, Y.G.; Fitzsimmons, K.E.; Chen, X.; Prud'homme, C.; Zong, X. Origin of loess deposits in the North Tian Shan piedmont, Central Asia. *Palaeogeogr. Palaeoclimatol. Palaeoecol.* **2020**, *559*, 109972. [CrossRef]
29. Miao, X.D.; Chongyi, E.; Xu, S.J.; Wang, Q.; Hanson, P.R.; Chen, H.; Shi, Y. Age and source of coastal loess in Shandong Peninsula, Bohai Sea, China: Implications for dust aggradation in respond to sea-level change. *Aeolian Res.* **2022**, *54*, 100767. [CrossRef]
30. Saimaiti, A.; Fu, C.F.; Song, Y.G.; Shukurov, N. Spatial Distribution, Material Composition and Provenance of Loess in Xinjiang, China: Progress and Challenges. *Atmosphere* **2022**, *13*, 1790. [CrossRef]
31. Stevens, T.; Adamiec, G.; Bird, A.F.; Lu, H. An abrupt shift in dust source on the Chinese Loess Plateau revealed through high sampling resolution OSL dating. *Quat. Sci. Rev.* **2013**, *82*, 121–132. [CrossRef]
32. Jin, X.L.; Zheng, K.Y. Geological initial observation of Miaodao Islands. *Oceanol. Limnol. Sin.* **1964**, *6*, 364–370.
33. Zhao, Q.H. A restudy of microfossils of the loess in Miaodao Islands, Bohai Sea. *Sci. China (Ser. D)* **1996**, *26*, 445–451.
34. Chen, H.T.; Kong, F.B.; Xu, S.J.; Lou, Z.; Zhang, J. Geochemical characteristics of major elements and their paleoenvironmental significance of the Xianjingyuan loess in Shandong Province. *Mar. Geol. Quat. Geol.* **2020**, *40*, 189–197.
35. Cheng, Z.B.; Fu, M.Z.; Ju, X.H. Geological significance of paleontological fossils in coastal loess in the Bohai Strait and Liaodong Peninsula. *Mar. Geol. Quat. Geol.* **1996**, *16*, 85–94.

36. Xu, S.J. Grain size characteristics and its indications of loess in Miaodao Islands, Shandong Province. *Mar. Sci.* **2008**, *32*, 60–63. [CrossRef]
37. Cao, J.X.; Liu, G.N.; Shi, N.; Chang, Y.; Song, C.; Yuan, H.; Guo, X. Holocene loess of Miaodao Islands in Shandong. *Quat. Sci.* **1993**, *13*, 25–33.
38. Cao, J.X.; Li, P.Y.; Shi, N. Loesses on Miaodao Islands, Shandong Province. *Sci. China (Ser. B)* **1987**, *4*, 111–1122.
39. Wang, X.F. Magnetism and Environment Information Analysis of Loess Stratum in Miaodao Islands. Master's Thesis, East China Normal University, Shanghai, China, 2007.
40. Xu, S.J.; Kong, F.B.; Jia, G.J.; Miao, X.; Ding, X. An integrated OSL chronology, sedimentology and geochemical approach to loess deposits from Tuoji Island, Shandong Province: Implications for the late quaternary paleoenvironment in East China. *Aeolian Res.* **2018**, *31*, 105–116. [CrossRef]
41. Ni, Z.C. Optically Stimulated Luminescence Dating and the Provenance Analysis of Loess in Miaodao Islands, Shandong Province. Master's Thesis, Shandong Normal University, Jinan, China, 2015.
42. Xu, S.J.; Ding, X.C.; Yu, L.P.; Ni, Z. Palaeoclimatic implications of aeolian sediments on the Miaodao Islands, Bohai Sea, East China, based on OSL dating and proxies. *Aeolian Res.* **2015**, *19*, 259–266. [CrossRef]
43. Lin, X.; Liu, J.; Wu, Z.H.; Liu, W.M.; Li, C.A.; Li, Z.W.; Wang, S.; Liu, H.; Chen, J. Provenance of the Loess in Shandong Province (Eastern China) during the Last Ice Age: Constraints from the U-Pb Age of Detrital Zircons. *Earth Sci.* **2021**, *46*, 3230–3244. (In Chinese with English Abstract). [CrossRef]
44. Ding, X.C.; Cao, W.; Xu, S.J.; Kong, F.; Miao, X. The sedimentary characteristics of Dakoubei loess profile in Tuoji island and their palaeoenvironment significance. *J. Arid. Land Resour. Environ.* **2016**, *30*, 192–197.
45. Liu, J.P.; Zhao, S.L. Origin of the buried loess in the Bohai Sea bottom and the exposed loess along the coastal zone. *Oceanol. Limnol. Sin.* **1995**, *26*, 363–368.
46. Tian, S.C.; Sun, J.M.; Lü, L.X.; Cao, M.; Zhang, Z.; Lü, T. Optically stimulated luminescence dating of late Quaternary loess deposits in the coastal region of North China: Provenance and paleoclimatic implications. *Quat. Sci. Rev.* **2019**, *218*, 160–177. [CrossRef]
47. Zhu, Y.F.; Yin, Y.H.; Yu, H.S. In Genesis and Landscape Comprehensive Evaluation of Unique Marine Geological Relics in Changdao Islands. In Proceedings of the 20th Annual Conference of Tourism Geoscience and Geoparks of China Geological Society, Beijing, China, June 2005; pp. 94–100.
48. Cao, Y.L.; Wang, K.F.; Chen, H.T.; Xu, Y.; Zhang, C.; Wu, B.; Wang, Z.; Song, Y.; Xu, S.; Zhang, T.; et al. Spatial transport characteristics of dust indicated by end-members of grain size of loess in Miaodao Islands. *J. Sea Res.* **2023**, *192*, 102328. [CrossRef]
49. Muhs, D.R. Origins and Properties of Quaternary Loess Deposits. In *Reference Module in Earth Systems and Environmental Sciences*; Elsevier: Amsterdam, The Netherlands, 2014; ISBN 978-0-12-409548-9.
50. Bronger, A.; Heinkele, T. Mineralogical and clay mineralogical aspects of loess research. *Quat. Int.* **1990**, *7–8*, 37–51. [CrossRef]
51. Muhs, D.R. The geochemistry of loess: Asian and North American deposits compared. *J Asian Earth Sci.* **2018**, *155*, 81–115. [CrossRef]
52. Zhao, K.H. The Origin of the Loess in the Chain Islands of Miao—A Mineralogic View. *Mar. Sci.* **1983**, *8*, 29–32.
53. Seyedrahimi-Niaraq, M.; Mahdiyanfar, H. Introducing a new approach of geochemical anomaly intensity index (GAII) for increasing the probability of exploration of shear zone gold mineralization. *Geochemistry* **2021**, *81*, 125830. [CrossRef]
54. Seyedrahimi-Niaraq, M.; Mahdiyanfar, H. Improvement of geochemical prospectivity mapping using power spectrum; area fractal modeling of multi-element mineralization factor (SAF-MF). *Geochem. Explor. Environ. Anal.* **2022**, *22*, geochem2022-015. [CrossRef]
55. Chen, J.; Ji, J.F.; Qiu, G.; Zhu, H.B.; Lu, H.Y. Geochemical study on chemical weathering degree of loess in Luochuan, Shanxi Province. *Sci. China (Ser. D)* **1997**, *27*, 531–536.
56. Xu, S.J.; Ni, Z.C.; Ding, X.C. Geochemical Characteristics of Major Elements of the Pingyin Loess in Shandong Province. *Bull. Mineral. Petrol. Geochem.* **2016**, *35*, 353–359.
57. Chen, Y.Y.; Li, X.S.; Han, Z.Y.; Yang, S.; Wang, Y.; Yang, D. Chemical weathering intensity and element migration features of the Xiashu loess profile in Zhenjiang, Jiangsu Province. *J. Geogr. Sci.* **2008**, *18*, 341–352. [CrossRef]
58. Taylor, S.R.; McLennan, S.M.; McCulloch, M.T. Geochemistry of loess, continental crustal composition and crustal model ages. *Geochim. Cosmochim. Acta* **1983**, *47*, 1897–1905. [CrossRef]
59. Gallet, S.; Jahn, B.; Torii, M. Geochemical characterization of the Luochuan loess-paleosol sequence, China, and paleoclimatic implications. *Chem. Geol.* **1996**, *133*, 67–88. [CrossRef]
60. Jahn, B.; Gallet, S.; Han, J. Geochemistry of the Xining, Xifeng and Jixian sections, Loess Plateau of China: Eolian dust provenance and paleosol evolution during the last 140 ka. *Chem. Geol.* **2001**, *178*, 71–94. [CrossRef]
61. Fu, X.H. Geochemical Characteristics of Pingyin Loess and Its Provenance in Shandong Province. Master's Thesis, Shandong Normal University, Jinan, China, 2014.
62. Ding, Z.L.; Sun, J.M.; Yang, S.L.; Liu, T.S. Geochemistry of the Pliocene red clay formation in the Chinese Loess Plateau and implications for its origin, source provenance and paleoclimate change. *Geochim. Cosmochim. Acta* **2001**, *65*, 901–913. [CrossRef]
63. Nesbitt, H.W.; Young, G.M. Early Proterozoic climates and plate motions inferred from major element chemistry of lutites. *Nature* **1982**, *299*, 715–717. [CrossRef]

64. Qiao, Y.S.; Hao, Q.Z.; Peng, S.S.; Wang, Y.; Li, J.; Liu, Z. Geochemical characteristics of the eolian deposits in southern China, and their implications for provenance and weathering intensity. *Palaeogeogr. Palaeoclimatol. Palaeoecol.* **2011**, *308*, 513–523. [CrossRef]
65. Fedo, C.M.; Nesbitt, H.W.; Young, G.M. Unraveling the effects of potassium metasomatism in sedimentary rocks and paleosols, with implications for paleoweathering conditions and provenance. *Geology* **1995**, *23*, 921–924. [CrossRef]
66. McLennan, S.M. Weathering and global denudation. *J. Geol.* **1993**, *101*, 295–303. [CrossRef]
67. Wang, P.; Du, Y.; Yu, W.; Algeo, T.J.; Zhou, Q.; Xu, Y.; Qi, L.; Yuan, L.; Pan, W. The chemical index of alteration (CIA) as a proxy for climate change during glacial-interglacial transitions in Earth history. *Earth-Sci. Rev.* **2020**, *201*, 103032. [CrossRef]
68. Zhuang, W.; Dong, Y.W.; Yu, Y.; Liu, B.; Li, Y.; Li, Y.; Wang, M. Chemical weathering of the loess in the south of Liaoning Province and its implications for environmental change. *Mar. Geol. Quat. Geol.* **2013**, *33*, 163–171. [CrossRef]
69. Gu, Z.Y.; Lal, D.; Liu, T.S.; Guo, Z.T.; Southon, J.; Caffee, M.W. Weathering histories of Chinese loess deposits based on uranium and thorium series nuclides and cosmogenic 10Be. *Geochim. Cosmochim. Acta* **1997**, *61*, 5221–5231. [CrossRef]
70. Peng, S.Z.; Hao, Q.Z.; Wang, L.; Ding, M.; Zhang, W.; Wang, Y.; Guo, Z. Geochemical and grain-size evidence for the provenance of loess deposits in the Central Shandong Mountains region, northern China. *Quat. Res.* **2016**, *85*, 290–298. [CrossRef]
71. Robert Minard Garrels; Mackenzie, F.T. *Evolution of Sedimentary Rocks*; Norton: New York, NY, USA, 1971; p. 397. ISBN 0393099598.
72. Xie, Y.Y.; Chi, Y.P. Geochemical investigation of dry- and wet-deposited dust during the same dust-storm event in Harbin, China: Constraint on provenance and implications for formation of aeolian loess. *J. Asian Earth Sci.* **2016**, *120*, 43–61. [CrossRef]
73. Zhang, H.; Lu, H.; Jiang, S.; Vandenberghe, J.; Wang, S.; Cosgrove, R. Provenance of loess deposits in the Eastern Qinling Mountains (central China) and their implications for the paleoenvironment. *Quat. Sci. Rev.* **2012**, *43*, 94–102. [CrossRef]
74. Sun, J.M.; Li, S.H.; Muhs, D.R.; Li, B. Loess sedimentation in Tibet: Provenance, processes, and link with Quaternary glaciations. *Quat. Sci. Rev.* **2007**, *26*, 2265–2280. [CrossRef]
75. Li, Y.; Song, Y.G.; Chen, X.L.; Li, J.; Mamadjanov, Y.; Aminov, J. Geochemical composition of Tajikistan loess and its provenance implications. *Palaeogeogr. Palaeoclimatol. Palaeoecol.* **2016**, *446*, 186–194. [CrossRef]
76. Taylor, S.R.; McLennan, S.M. *The Continental Crust: Its Composition and Evolution. An Examination of the Geochemical Record Preserved in Sedimentary Rocks*; Blackwell Scientific Publishing: Oxford, UK, 1985; pp. 1–312.
77. McLennan, S.M. Relationships between the trace element composition of sedimentary rocks and upper continental crust. *Geochem. Geophys. Geosystems G3* **2001**, *2*, 2000G–2109G. [CrossRef]
78. Amorosi, A.; Centineo, M.C.; Dinelli, E.; Lucchini, F.; Tateo, F. Geochemical and mineralogical variations as indicators of provenance changes in late Quaternary deposits of SE Po Plain. *Sediment. Geol.* **2002**, *151*, 273–292. [CrossRef]
79. Mikes, T.; Dunkl, I.; Frisch, W.; von Eynatten, H. Geochemistry of Eocene flysch sandstones in the NW External Dinarides. *Acta Geol. Hung.* **2006**, *49*, 103–124. [CrossRef]
80. Condie, K.C. Chemical composition and evolution of the upper continental crust: Contrasting results from surface samples and shales. *Chem. Geol.* **1993**, *104*, 1–37. [CrossRef]
81. Floyd, P.A.; Winchester, J.A.; Park, R.G. Geochemistry and tectonic setting of Lewisian clastic metasediments of the early Proterozoic Loch Maree Group of Gairloch, NW Scotland. *Precambrian Res.* **1989**, *45*, 203–214. [CrossRef]
82. Sun, J.M. Provenance of loess material and formation of loess deposits on the Chinese Loess Plateau. *Earth Planet Sci. Lett.* **2002**, *203*, 845–859. [CrossRef]
83. Hiscott, R.N. Ophiolitic source rocks for Taconic-age flysch: Trace-element evidence. *GSA Bull.* **1984**, *95*, 1261–1267. [CrossRef]
84. Rudnick, R.L.; Gao, S. *Composition of the Continental Crust. Treatise Geochem 3:1-64*; Elsevier: Amsterdam, The Netherlands, 2003.
85. Anders, E.; Grevesse, N. Abundances of the elements: Meteoritic and solar. *Geochim. Cosmochim. Acta* **1989**, *53*, 197–214. [CrossRef]
86. McLennan, S.M.; Lipin, B.R.; McKay, G.A. Rare earth elements in sedimentary rocks; influence of provenance and sedimentary processes. *Rev. Mineral.* **1989**, *21*, 169–200.
87. Hu, F.; Yang, X. Geochemical and geomorphological evidence for the provenance of aeolian deposits in the Badain Jaran Desert, northwestern China. *Quat. Sci. Rev.* **2016**, *131*, 179–192. [CrossRef]